


Superaligned $0^+ \rightarrow 0^+$ nuclear β decays: 2020 critical survey, with implications for V_{ud} and CKM unitarity

J. C. Hardy^{*} and I. S. Towner

Cyclotron Institute, Texas A&M University, College Station, Texas 77843, USA

 (Received 18 March 2020; accepted 25 August 2020; published 2 October 2020)

A new critical survey of all half-life, decay-energy, and branching-ratio measurements related to 23 superallowed $0^+ \rightarrow 0^+$ β decays is presented. Included are 222 individual measurements of comparable precision obtained from 174 published references. Compared with our last survey in 2015, we have added results from 28 new publications and eliminated an approximately equal number whose results have been superseded by much more precise modern data. We obtain world-average ft values for each of the 21 transitions that have a complete set of data and then apply radiative and isospin-symmetry-breaking corrections to extract “corrected” $\mathcal{F}t$ values. Fifteen of these $\mathcal{F}t$ values now have a precision of 0.3% or better and all take the same value within statistics, as expected from conservation of the vector current. Their average, $\overline{\mathcal{F}t}$, when combined with the muon lifetime, yields the up-down quark-mixing element of the Cabibbo-Kobayashi-Maskawa matrix, $V_{ud} = 0.97373 \pm 0.00031$. This is lower than our 2015 result by one standard deviation and its uncertainty is increased by 50%. This is a consequence not of any shifts in the experimental data but of new calculations for the radiative corrections. The lower V_{ud} value now leads to greater tension in the top-row test of unitarity in the CKM matrix. Updates in experimental data have independently led to a factor-of-two tighter limit being set on the possible existence of a scalar interaction. The new limit on Fierz interference is $b_F \leq 0.0033$ at the 90% confidence level.

DOI: [10.1103/PhysRevC.102.045501](https://doi.org/10.1103/PhysRevC.102.045501)

I. INTRODUCTION

The study of $0^+ \rightarrow 0^+$ nuclear β decays plays an important role in our current understanding of the electroweak interaction. These transitions are now well known in the decays of a wide range of nuclei from ^{10}C to ^{74}Rb . Considered together, they probe the conservation of the vector current, set tight limits on the possible presence of scalar currents, and provide the most precise value for V_{ud} , the up-down quark-mixing element of the Cabibbo-Kobayashi-Maskawa (CKM) matrix. This latter result has become a linchpin in the most demanding available test of the unitarity of the CKM matrix: that the sum of squares of the top-row elements should equal unity.

We have published seven previous surveys of $0^+ \rightarrow 0^+$ superallowed transitions [1–7], the first having appeared 47 years ago and the most recent 5 years ago. In this, the eighth, we follow the same approach. We present a complete catalog of all the relevant world data pertaining to these superallowed transitions, laying out our criteria for inclusion and explaining clearly our reasons, case by case, for any rejections. It is quite remarkable that over five decades, as experimental techniques have evolved substantially, the experimental ft values have formed a very robust set of data. Collectively their precision has steadily improved, while their central values have changed but little.

Since our last survey closed in September 2014, there has continued to be a great deal of activity in the field, both in experiment and in theory. This review contains 28 new experimental references, while an approximately equal number of older references have been dropped because their uncertainties were more than 10 times larger than some new measurement. On the theory side, activity has focused on radiative corrections, the source of the largest contribution to the uncertainty in V_{ud} . New calculations have resulted in a lowering of the value of V_{ud} but with a concomitant increase in its uncertainty. This increase is unfortunate since it renders the test of CKM unitarity less definitive. The reduction in V_{ud} creates considerable tension in the unitarity sum, but the increase in its uncertainty makes a definite conclusion elusive.

Overall, recent improvements have been numerous and important enough that we consider this to be an opportune time to produce a new and updated survey. The number of separate transitions itemized has increased from 20 to 23, and the number whose ft -value precision is 0.23% or better has risen to 15, principally due to successful, yet demanding, branching-ratio measurements. We continue the practice begun in 1984 [3] of updating all original data to take account of the most modern calibration standards. There are fewer data remaining in the data base these days requiring such updates, especially for the Q_{EC} values, where recent Penning trap results are dominating the field.

Since the axial current cannot contribute in first order to transitions between spin-0 states, superallowed $0^+ \rightarrow 0^+$ β decay between $T = 1$ analog states depends uniquely on the vector part of the weak interaction. Thus, according to the

^{*}hardy@comp.tamu.edu

conserved vector current (CVC) hypothesis, the experimental ft value for such a transition should be directly related to the vector coupling constant, G_V , a fundamental constant, which must be the same for all such transitions.

In practice, the ft values are subject to several small ($\sim 1\%$) correction terms. It is convenient to combine some of these terms with the ft value and define a “corrected” $\mathcal{F}t$ value, which replaces ft in satisfying the CVC expectations. Thus, we write [7]

$$\mathcal{F}t \equiv ft(1 + \delta'_R)(1 + \delta_{NS} - \delta_C) = \frac{K}{2G_V^2(1 + \Delta_R^V)}, \quad (1)$$

where $K/(\hbar c)^6 = 2\pi^3 \hbar \ln 2 / (m_e c^2)^5 = 8120.27648(26) \times 10^{-10} \text{ GeV}^{-4}\text{s}$, G_V is the vector coupling constant for semileptonic weak interactions, δ_C is the isospin-symmetry-breaking correction, and Δ_R^V is the transition-independent part of the radiative correction. The terms δ'_R and δ_{NS} comprise the transition-dependent part of the radiative correction, the former being a function only of the electron’s energy and the Z of the daughter nucleus, while the latter, like δ_C , depends in its evaluation on the details of nuclear structure. From this equation, it can be seen that each measured transition establishes an individual value for G_V and, if G_V is not renormalized in the nuclear medium as CVC asserts it is not, all such values—and all the $\mathcal{F}t$ values themselves—should be identical within uncertainties, regardless of the specific nuclei involved.

What makes the study of superallowed $0^+ \rightarrow 0^+$ β decays so compelling is that their precisely determined $\mathcal{F}t$ values have proved indeed to be consistent with one another. Thus their average yields an even more precise value for the vector coupling constant G_V , which in turn can be used to determine V_{ud} via the relation

$$V_{ud} = G_V / G_F, \quad (2)$$

where G_F is the well-known weak-interaction constant for muon decay. Once the value of V_{ud} is established it can be used to test the top-row unitarity of the CKM matrix, i.e., asking whether $V_{ud}^2 + V_{us}^2 + V_{ub}^2$ equals 1. For the past decade and more, the answer has consistently been “yes” but recent theoretical developments have made the answer today more ambiguous. We will present the current status of CKM unitarity.

Our procedure in this paper is to examine all experimental data related to 23 superallowed transitions, comprising all those that have been well studied, together with other cases that are now coming under scrutiny after becoming accessible to precision measurement in relatively recent years. The methods used in data evaluation are presented in Sec. II along with tables of all the relevant world data. The calculations and corrections required to extract $\mathcal{F}t$ values from these data are described and applied in Sec. III. Then in Sec. IV we examine the resultant $\mathcal{F}t$ values, their consistency, and their constituent uncertainties. Finally, in Sec. V we explore the impact of these results on two weak-interaction issues: CKM unitarity and the possible existence of scalar interactions. This is much the same pattern as we followed in our three most recent reviews [5–7].

II. EXPERIMENTAL DATA

The ft value that characterizes any β transition depends on three measured quantities: the total transition energy Q_{EC} , the half-life $t_{1/2}$ of the parent state, and the branching ratio R for the particular transition of interest. The Q_{EC} value is required to determine the statistical rate function, f , while the half-life and branching ratio combine to yield the partial half-life, t . In Tables I–VII we present the measured values of these three quantities and supporting information for a total of 23 superallowed $0^+ \rightarrow 0^+$ transitions. Of these 23 transitions, 15 have been fully characterized by precise measurements; their ft values are currently known with a relative precision of $\pm 0.23\%$ or better, and they all play a role in important weak-interaction tests to be described in later sections.

The remaining eight transitions are much less well known for now, but they are accessible to experiment and their data could be significantly improved in future. We include them for completeness and to encourage their further study. There are, of course, even more $0^+ \rightarrow 0^+$ transitions that are known or anticipated to exist. However, we omit them entirely because their parents are exotic enough that we consider it unlikely they could be precisely characterized in the foreseeable future.

A. Evaluation principles

In our treatment of the data, we considered all measurements formally published or accepted before the end of March 2020. We scrutinized all the original experimental reports in detail. Where necessary and possible, we used the information provided there to correct the results for calibration data that have improved since the measurement was made. All cases for which such a correction has been made are recorded in Table VI. If corrections were evidently required but insufficient information was provided to make them, then the results were rejected; these are noted in Table VII.

Of the surviving results, only those with (updated) uncertainties that are within a factor of 10 of the most precise measurement for each quantity were retained for averaging in the tables. Each datum appearing in the tables is attributed to its original journal reference *via* an alphanumeric code comprising the initial two letters of the first author’s name and the two last digits of the publication date. These codes are correlated with the actual reference numbers [8–181] in Table VIII.

The statistical procedures we have followed in analyzing the tabulated data are based on those used by the Particle Data Group in their periodic reviews of particle properties, e.g., see Ref. [182], and adopted by us in earlier surveys [1–7] of superallowed $0^+ \rightarrow 0^+$ β decay. In the tables and throughout this work, “error bars” and “uncertainties” always refer to plus-and-minus one standard deviation (68% confidence level). For a set of N uncoupled measurements, $x_i \pm \delta x_i$, of a particular quantity, a Gaussian distribution is assumed, the weighted average being calculated according to:

$$\bar{x} \pm \delta \bar{x} = \frac{\sum_i w_i x_i}{\sum_i w_i} \pm (\sum_i w_i)^{-1/2}, \quad (3)$$

TABLE I. Measured results from which the decay transition energies, Q_{EC} , have been derived for superallowed β decays. The lines giving the average superallowed Q_{EC} values themselves are in bold. (See Table VIII for the correlation between the alphanumeric reference code used in this table and the actual reference numbers.)

Parent/daughter nuclei	property ^a	Measured energies used to determine Q_{EC} (keV)			Average value		
		1	2	3	Energy (keV)	Scale	
$T_z = -1$							
¹⁰ C	¹⁰ B	$Q_{EC}(gs)$	3647.83 ± 0.34 [Ba84]	3647.95 ± 0.12 [Ba98]	3648.12 ± 0.08 [Er11]		
			3648.34 ± 0.51 [Kw13]			3648.063 ± 0.064	1.0
		$E_x(d0^+)$	1740.15 ± 0.17 [Aj88]	1740.068 ± 0.017 ^b		1740.069 ± 0.017	1.0
	$Q_{EC}(sa)$				1907.994 ± 0.067		
¹⁴ O	¹⁴ N	$Q_{EC}(gs)$	5144.33 ± 0.17 [To03]	5144.364 ± 0.025 [Va15]		5144.363 ± 0.025	1.0
		$E_x(d0^+)$	2312.798 ± 0.011 [Aj91]			2312.798 ± 0.011	
		$Q_{EC}(sa)$				2831.543 ± 0.076^c	2.8
¹⁸ Ne	¹⁸ F	ME(p)	5316.8 ± 1.5 [Ma94]	5317.63 ± 0.36 [Bl04b]		5317.58 ± 0.35	1.0
		ME(d)	871.99 ± 0.73 [Bo64]	874.2 ± 2.2 [Ho64]	875.2 ± 2.8 [Pr67]		
			877.2 ± 3.0 [Se73]	874.01 ± 0.60 [Ro75]		873.37 ± 0.59	1.3
		$Q_{EC}(gs)$				4444.21 ± 0.68	
		$E_x(d0^+)$	1041.55 ± 0.08 [Bc77]			1041.55 ± 0.08	
	$Q_{EC}(sa)$				3402.66 ± 0.69		
²² Mg	²² Na	$Q_{EC}(gs)$	4781.64 ± 0.28 [Mu04]	4781.40 ± 0.67 [Sa04]	4781.40 ± 0.22 [Re17]	4781.49 ± 0.17	1.0
		$E_x(d0^+)$	657.00 ± 0.14 [Wa67]			657.00 ± 0.14	
		$Q_{EC}(sa)$				4124.49 ± 0.22	
²⁶ Si	²⁶ Al	$Q_{EC}(sa)$	4840.85 ± 0.10 [Er09a]			4840.85 ± 0.10	
³⁰ S	³⁰ P	$Q_{EC}(gs)$	6141.61 ± 0.19 [So11]			6141.61 ± 0.19	
		$E_x(d0^+)$	677.01 ± 0.03 [Gr00]			677.01 ± 0.03	
		$Q_{EC}(sa)$				5464.60 ± 0.19	
³⁴ Ar	³⁴ Cl	$Q_{EC}(sa)$	6061.83 ± 0.08 [Er11]			6061.83 ± 0.08	
³⁸ Ca	³⁸ K	$Q_{EC}(sa)$	6612.12 ± 0.07 [Er11]			6612.12 ± 0.07	
⁴² Ti	⁴² Sc	$Q_{EC}(sa)$	7016.81 ± 0.25 [Ku09]			7016.81 ± 0.25	
⁴⁶ Cr	⁴⁶ V	ME(p)	-29474 ± 20 [Zi72]	-29471 ± 11 ^d		-29472 ± 10	1.0
		ME(d0 ⁺)	-37075.35 ± 0.19 ^e			-37075.35 ± 0.19	
		$Q_{EC}(sa)$				7604 ± 10	
⁵⁰ Fe	⁵⁰ Mn	ME(p)	-34489 ± 60 [Tr77]	-34477 ± 6 ^d		-34477 ± 6	1.0
		ME(d0 ⁺)	-42627.65 ± 0.41 ^e			-42627.65 ± 0.41	
		$Q_{EC}(sa)$				8151 ± 6	
⁵⁴ Ni	⁵⁴ Co	ME(p)	-39223 ± 50 [Tr77]	-39278 ± 4 ^d		-39278 ± 4	1.1
		ME(d0 ⁺)	-48010.12 ± 0.48 ^e			-48010.12 ± 0.48	
		$Q_{EC}(sa)$				8732 ± 4	
$T_z = 0$							
^{26m} Al	²⁶ Mg	$Q_{EC}(gs)$	4004.79 ± 0.55 [De69]	4004.41 ± 0.10 ^f	4004.36 ± 0.22 [Ge08]	4004.413 ± 0.089	1.0
		$E_x(p0^+)$	228.305 ± 0.013 [Al82]			228.305 ± 0.013	
		$Q_{EC}(sa)$	4232.19 ± 0.12 [Br94]	4232.83 ± 0.13 [Er06b]		4232.72 ± 0.15^e	2.7
³⁴ Cl	³⁴ S	$Q_{EC}(sa)$	5491.65 ± 0.26 ^g	5491.662 ± 0.047 [Er09b]		5491.662 ± 0.046	1.0
^{38m} K	³⁸ Ar	$Q_{EC}(sa)$	6044.38 ± 0.12 [Ha98]	6044.223 ± 0.041 [Er09b]		6044.240 ± 0.048	1.2
⁴² Sc	⁴² Ca	$Q_{EC}(sa)$	6425.84 ± 0.17 ^h	6426.13 ± 0.21 [Er06b]	6426.350 ± 0.053 [Er17]	6426.34 ± 0.12^e	2.5
⁴⁶ V	⁴⁶ Ti	$Q_{EC}(sa)$	7052.90 ± 0.40 [Sa05]	7052.72 ± 0.31 [Er06b]	7052.11 ± 0.27 [Fa09]		
			7052.44 ± 0.10 [Er11]			7052.45 ± 0.10	1.1
⁵⁰ Mn	⁵⁰ Cr	$Q_{EC}(sa)$	7634.48 ± 0.07 [Er08]			7634.453 ± 0.066^c	1.0
⁵⁴ Co	⁵⁴ Fe	$Q_{EC}(sa)$	8244.54 ± 0.10 [Er08]			8244.38 ± 0.26^e	3.2
⁶² Ga	⁶² Zn	$Q_{EC}(sa)$	9181.07 ± 0.54 [Er06a]			9181.07 ± 0.54	

TABLE I. (Continued).

Parent/daughter nuclei		property ^a	Measured energies used to determine Q_{EC} (keV)			Average value	
nuclei			1	2	3	Energy (keV)	Scale
⁶⁶ As	⁶⁶ Ge	ME(p)	-52018 ± 30 [Sc07]			-52018 ± 30	
		ME(d)	-61607.0 ± 2.4 [Sc07]			-61607.0 ± 2.4	
		Q_{EC} (sa)	9550 ± 50 [Da80]			9579 ± 26	1.0
⁷⁰ Br	⁷⁰ Se	Q_{EC} (sa)	9970 ± 170 [Da80]			9970 ± 170	
⁷⁴ Rb	⁷⁴ Kr	ME(p)	-51905 ± 18 [He02]	-51915.2 ± 4.0 [Ke07]	-51916.5 ± 6.0 [Et11]	-51915.2 ± 3.3	1.0
		ME(d)	-62332.0 ± 2.1 [Ro06]			-62332.0 ± 2.1	
		Q_{EC} (sa)				10416.8 ± 3.9	

^aAbbreviations used in this column are as follows: gs, transition between ground states; sa, superallowed transition; p, parent; d, daughter; ME, mass excess; $E_x(0^+)$, excitation energy of the 0^+ (analog) state. Thus, for example, “ Q_{EC} (sa)” signifies the Q_{EC} value for the superallowed transition, ME(d), the mass excess of the daughter nucleus; and ME($d0^+$), the mass excess of the daughter’s 0^+ state.

^bResult based on references [Ba88] and [Ba89].

^cAverage result includes the results of Q_{EC} pairs; see Table II.

^dResult based on references [Zh17] and [Zh18].

^eResult obtained from the Q_{EC} value for the superallowed decay of $d0^+$, which appears elsewhere in this table, combined with the mass of its daughter taken from [Wa17].

^fResult based on references [Is80], [Al82], [Hu82], [Be85], [Pr90], [Ki91], and [Wa92].

^gResult based on references [Wa83], [Ra83], and [Li94].

^hResult based on references [Zi87] and [Ki89].

where

$$w_i = 1/(\delta x_i)^2$$

and the sums extend over all N measurements.

For each average, the χ^2 is also calculated and a scale factor, S , determined:

$$S = [\chi^2/(N - 1)]^{1/2}, \tag{4}$$

where

$$\chi^2 = \sum_i \left(\frac{x_i - \bar{x}}{\delta x_i} \right)^2.$$

This factor is then used to establish the quoted uncertainty. If $S \leq 1$, then the value of $\delta\bar{x}$ from Eq. (3) is left unchanged. If $S > 1$ and the input δx_i are all about the same size, then we increase $\delta\bar{x}$ by the factor S , which is equivalent to assuming that all the experimental errors were underestimated by the same factor. Finally, if $S > 1$ but the δx_i are of widely varying

magnitudes, then S is recalculated with only those results for which $\delta x_i \leq 3N^{1/2}\delta\bar{x}$ being retained; the recalculated scale factor is then applied in the usual way. In all three cases, no change is made to the original average \bar{x} calculated with Eq. (3).

The data for Q_{EC} include measurements of both individual Q_{EC} values and the differences between pairs of Q_{EC} values. This required a two-step analysis procedure. We first treated the individual Q_{EC} -value measurements for each particular transition in the manner already described, obtaining an average result with uncertainty in each case, $\bar{x}_j \pm \delta\bar{x}_j$, where the subscript j now designates a particular transition. For transitions unconnected by difference measurements, these uncertainties were scaled if necessary and then the values were quoted as final results. For those transitions involved in one or more difference measurements we combined their average Q_{EC} values, $\bar{x}_j \pm \delta\bar{x}_j$, with the difference measurements, $d_k \pm \delta d_k$, in a single fitting procedure. If M_1 is the number of transitions that are connected by difference measurements,

TABLE II. Q_{EC} -value differences for superallowed β -decay branches. These data are also used as input to determine some of the average Q_{EC} values listed in Table I. (See Table VIII for the correlation between the alphabetical reference code used in this table and the actual reference numbers.)

Parent nucleus 1	Parent nucleus 2	$Q_{EC2} - Q_{EC1}$ (keV)	
		Measurement	Average ^a
¹⁴ O	^{26m} Al	1401.68 ± 0.13 [Ko87]	1401.17 ± 0.16
^{26m} Al	⁴² Sc	2193.5 ± 0.2 [Ko87]	2193.62 ± 0.19
⁴² Sc	⁵⁰ Mn	1207.6 ± 2.3 [Ha74d]	1208.12 ± 0.14
⁴² Sc	⁵⁴ Co	1817.2 ± 0.2 [Ko87]	1818.05 ± 0.28
⁵⁰ Mn	⁵⁴ Co	610.09 ± 0.17 [Ko87,Ko97b]	609.93 ± 0.27

^aAverage values include the results of direct Q_{EC} -value measurements; see Table I.

TABLE III. Half-lives, $t_{1/2}$, of superallowed β emitters. (See Table VIII for the correlation between the alphabetical reference code used in this table and the actual reference numbers.)

Parent nucleus	Measured half-lives, $t_{1/2}$ (ms)				Average value	
	1	2	3	4	$t_{1/2}$ (ms)	Scale
$T_z = -1$						
^{10}C	19295 \pm 15 [Ba90] 19300.9 \pm 1.7 [Du16]	19310 \pm 4 [Ia08]	19282 \pm 11 [Ba09]	19296.9 \pm 7.4 [Du16]	19301.6 \pm 2.4	1.6
^{14}O	70480 \pm 150 [Al72] 70613 \pm 25 [Wi78] 70623 \pm 53 [Ta12]	70588 \pm 28 [Cl73] 70560 \pm 49 [Ga01] 70610 \pm 30 [La13]	70430 \pm 180 [Az74] 70641 \pm 20 [Ba04] 70632 \pm 94 [La13]	70684 \pm 77 [Be78] 70696 \pm 52 [Bu06]	70619 \pm 11	1.0
^{18}Ne	1669 \pm 4 [Al75]	1664.8 \pm 1.1 [Gr13]	1664.00 \pm 0.53 [La15]		1664.22 \pm 0.47	1.0
^{22}Mg	3875.5 \pm 1.2 [Ha03]	3874.00 \pm 0.79 [Du17]			3874.45 \pm 0.69	1.0
^{26}Si	2245.3 \pm 0.7 [Ia10]				2245.3 \pm 0.7	
^{30}S	1175.9 \pm 1.7 [So11]	1179.92 \pm 0.34 [Ia18]			1179.77 \pm 0.77	2.3
^{34}Ar	844.5 \pm 3.4 [Ha74a]	846.46 \pm 0.35 [Ia19a]			846.44 \pm 0.35	1.0
^{38}Ca	443.8 \pm 1.9 [Bl10]	443.77 \pm 0.36 [Pa11]	443.63 \pm 0.35 [Bl15]		443.70 \pm 0.25	1.0
^{42}Ti	208.14 \pm 0.45 [Ku09]	211.7 \pm 1.9 [Mo15]			208.33 \pm 0.80	1.8
^{46}Cr	224.3 \pm 1.3 [Mo15]	223.9 \pm 9.9 [Mo15]			224.3 \pm 1.3	1.0
^{50}Fe	152.1 \pm 0.6 [Mo15]	150.1 \pm 2.9 [Mo15]			152.02 \pm 0.59	1.0
^{54}Ni	114.2 \pm 0.3 [Mo15]	114.3 \pm 1.8 [Mo15]			114.20 \pm 0.30	1.0
$T_z = 0$						
^{26m}Al	6346 \pm 5 [Fr69a] 6346.54 \pm 0.76 [Fi11]	6346 \pm 5 [Az75] 6347.8 \pm 2.5 [Sc11]	6339.5 \pm 4.5 [Al77] 6345.3 \pm 0.9 [Ch13]	6346.2 \pm 2.6 [Ko83]	6346.02 \pm 0.54	1.0
^{34}Cl	1526 \pm 2 [Ry73]	1525.2 \pm 1.1 [Wi76]	1527.7 \pm 2.2 [Ko83]	1526.8 \pm 0.5 [Ia06]	1526.55 \pm 0.44	1.0
^{38m}K	925.6 \pm 0.7 [Sq75] 924.4 \pm 0.6 [Ba00]	922.3 \pm 1.1 [Wi76] 924.46 \pm 0.14 [Ba10]	921.71 \pm 0.65 [Wi78]	924.15 \pm 0.31 [Ko83]	924.33 \pm 0.27	2.3
^{42}Sc	680.98 \pm 0.62 [Wi76]	680.67 \pm 0.28 [Ko97a]			680.72 \pm 0.26	1.0
^{46}V	422.47 \pm 0.39 [Al77]	422.28 \pm 0.23 [Ba77a]	422.57 \pm 0.13 [Ko97a]	422.66 \pm 0.06 [Pa12]	422.622 \pm 0.053	1.2
^{50}Mn	284.0 \pm 0.4 [Ha74b] 283.10 \pm 0.14 [Ba06]	282.8 \pm 0.3 [Fr75]	282.72 \pm 0.26 [Wi76]	283.29 \pm 0.08 [Ko97a]	283.21 \pm 0.11	1.7
^{54}Co	193.4 \pm 0.4 [Ha74b]	193.0 \pm 0.3 [Ho74]	193.28 \pm 0.18 [Al77]	193.28 \pm 0.07 [Ko97a]	193.271 \pm 0.063	1.0
^{62}Ga	115.84 \pm 0.25 [Hy03] 116.100 \pm 0.025 [Gr08]	116.19 \pm 0.04 [Bl04a]	116.09 \pm 0.17 [Ca05]	116.01 \pm 0.19 [Hy05]	116.121 \pm 0.040	1.9
^{66}As	95.78 \pm 0.39 [Al78]	95.77 \pm 0.28 [Bu88]	97 \pm 2 [Ji02]		95.79 \pm 0.23	1.0
^{70}Br	80.2 \pm 0.8 [Al78]	78.54 \pm 0.59 [Bu88]	78.42 \pm 0.51 [Mo17]		78.80 \pm 0.48	1.4
^{74}Rb	64.90 \pm 0.09 [Oi01]	64.761 \pm 0.031 [Ba01]			64.776 \pm 0.043	1.5

and M_2 is the number of those difference measurements, then we have a total of $M_1 + M_2$ input data values from which we need to extract a final set of M_1 average Q_{EC} values, $\bar{x}_j \pm \delta\bar{x}_j$. We accomplish this by minimizing χ^2 , where

$$\chi^2 = \sum_{j=1}^{M_1} \left(\frac{\tilde{x}_j - \bar{x}_j}{\delta\tilde{x}_j} \right)^2 + \sum_{k=1}^{M_2} \left(\frac{d_k - \bar{d}_k}{\delta d_k} \right)^2 \quad (5)$$

and

$$\bar{d}_k = \bar{x}_{j_1} - \bar{x}_{j_2},$$

with j_1 and j_2 designating the two transitions whose Q_{EC} value difference is determined in a particular d_k measurement. For each of these individual Q_{EC} values, we obtained its scale factor from Eq. (4), where the χ^2 used in that equation is now given by

$$\chi^2 = \sum_i \left(\frac{x_i - \bar{x}_j}{\delta x_i} \right)^2 + \sum_l \left(\frac{d_l - \bar{d}_l}{\delta d_l} \right)^2, \quad (6)$$

where j is the particular transition of interest. The sum in i extends over all individual Q_{EC} -value measurements of transition j , and the sum in l extends over all doublet measurements that include transition j as one component. The resultant value of S was applied to the uncertainty, $\delta\bar{x}_j$, with the same conventions as were described previously.

Overall, our evaluation procedures are very conservative. Unless there is a clearly identifiable reason to reject a result, we include it in our data base even if it deviates significantly from other measurements of the same quantity, the consequent nonstatistical spread in results being reflected in an increased (scaled) uncertainty assigned to the average. The corresponding scale factor S is listed in the ‘‘scale’’ column of the tables.¹ Of course there are also some results that must be rejected

¹Because S is used only to increase the uncertainty, S values that are calculated to be less than unity are recorded in the tables as $S = 1$ to indicate that no change has been made to the uncertainty.

TABLE IV. Measured results from which the branching ratios, R , have been derived for superallowed β transitions. The lines giving the average superallowed branching ratios themselves are in bold print. (See Table VIII for the correlation between the alphabetical reference code used in this table and the actual reference numbers.)

Parent/daughter nuclei	Daughter state E_x (MeV)	Measured branching ratio, R (%)		Average value		
		1	2	R (%)	Scale	
$T_z = -1$						
^{10}C	^{10}B	2.16	$0_{-0}^{+0.0008}$ [Go72]		$0_{-0}^{+0.0008}$	
		1.74	1.468 ± 0.014 [Ro72]	1.473 ± 0.007 [Na91]		
			1.465 ± 0.009 [Kr91]	1.4625 ± 0.0025 [Sa95]		
		1.4665 ± 0.0038 [Fu99]		1.4646 ± 0.0019	1.0	
^{14}O	^{14}N	gs	0.72 ± 0.06^a	0.55 ± 0.03^b		
			0.4934 ± 0.0073 [Vo15]		0.500 ± 0.013	1.9
		3.95	0.062 ± 0.007 [Ka69]	0.058 ± 0.004 [Wi80]		
			0.053 ± 0.002 [He81]		0.0545 ± 0.0019	1.1
				99.446 ± 0.013		
^{18}Ne	^{18}F	1.04	9 ± 3 [Fr63]	7.69 ± 0.21^c [Ha75]	7.70 ± 0.21	1.0
^{22}Mg	^{22}Na	0.66	54.0 ± 1.1 [Ha75]	53.15 ± 0.12 [Ha03]	53.16 ± 0.12	1.0
^{26}Si	^{26}Al	1.06	21.8 ± 0.8 [Ha75]	21.21 ± 0.64 [Ma08]	21.44 ± 0.50	1.0
		0.23	75.69 ± 0.14 [Be19]		75.67 ± 0.14^c	1.0
^{30}S	^{30}P	gs	20 ± 1 [Fr63]		20 ± 1	
		0.68			77.4 ± 1.0^c	
^{34}Ar	^{34}Cl	gs	94.44 ± 0.25 [Ha74a]	94.48 ± 0.08 [Ia19b]	94.476 ± 0.076	1.0
^{38}Ca	^{38}K	0.13	77.28 ± 0.16 [Pa14,Pa15]	77.14 ± 0.35 [B115]	77.26 ± 0.15	1.0
^{42}Ti	^{42}Sc	0.61	51.1 ± 1.1 [Ku09]	55.9 ± 3.6 [Mo15]	51.5 ± 1.3	1.3
		gs			48.1 ± 1.4^c	
^{46}Cr	^{46}V	0.99	21.6 ± 5.0 [On05]	13.9 ± 1.0 [Mo15]	14.2 ± 1.4	1.5
		gs			76.7 ± 2.3^c	
^{50}Fe	^{50}Mn	0.65	22.5 ± 1.4 [Mo15]		22.5 ± 1.4	
		gs			73.9 ± 1.7^c	
^{54}Ni	^{54}Co	0.94	22.4 ± 4.4 [Re99]	19.8 ± 1.2 [Mo15]	19.9 ± 1.2	1.0
		gs			78.9 ± 1.2^c	
$T_z = 0$						
^{26m}Al	^{26}Mg	gs	> 99.997 [Ki91]	> 99.9985 [Fi12]	$100.0000_{-0.0015}^{+0}$	
^{34}Cl	^{34}S	gs	> 99.988 [Dr75]		$100.000_{-0.012}^{+0}$	
^{38m}K	^{38}Ar	3.38	< 0.0019 [Ha94]	< 0.0008 [Le08]	$0.0000_{-0}^{+0.0008}$	
		gs (^{38}K) ^d	0.0330 ± 0.0043 [Le08]		0.0330 ± 0.0043	
		gs			$99.9670_{-0.0044}^{+0.0043}$	
^{42}Sc	^{42}Ca	1.84	0.0063 ± 0.0026 [In77]	0.0022 ± 0.0017 [De78]		
			0.0103 ± 0.0031 [Sa80]	0.0070 ± 0.0012 [Da85]	0.0059 ± 0.0014	1.6
		gs			99.9941 ± 0.0014	
^{46}V	^{46}Ti	2.61	0.0039 ± 0.0004 [Ha94]		0.0039 ± 0.0004	
		4.32	0.0113 ± 0.0012 [Ha94]		0.0113 ± 0.0012	
		ΣGT^e	< 0.01		$0.00_{-0}^{+0.01}$	
		gs			$99.9848_{-0.0100}^{+0.0013}$	
^{50}Mn	^{50}Cr	3.63	0.057 ± 0.003 [Ha94]		0.057 ± 0.003	
		3.85	< 0.0003 [Ha94]		$0.0000_{-0}^{+0.0003}$	
		5.00	0.0007 ± 0.0001 [Ha94]		0.0007 ± 0.0001	
		gs			99.9423 ± 0.0030	
^{54}Co	^{54}Fe	2.56	0.0045 ± 0.0006 [Ha94]		0.0045 ± 0.0006	
		ΣGT^e	< 0.03		$0.00_{-0}^{+0.03}$	
		gs			$99.9955_{-0.0300}^{+0.0006}$	
^{62}Ga	^{62}Zn	ΣGT^e	0.142 ± 0.008 [Fi08]	0.107 ± 0.024 [Be08]	0.139 ± 0.011	1.4
		gs			99.862 ± 0.011	
^{74}Rb	^{74}Kr	ΣGT^e	0.5 ± 0.1 [Pi03]	0.455 ± 0.031 [Du13]	0.459 ± 0.030	
		gs			99.541 ± 0.030	

^aResult based on Refs. [Fr63], [To05], and [Vo15].

^bResult based on Refs. [Si66], [To05], and [Vo15].

^cResult also incorporates data from Table V.

^dThe decay of ^{38m}K includes a weak γ -ray branch to the ^{38}K ground state, which competes with the β decay.

^eDesignates total Gamow-Teller transitions to levels not explicitly listed; in cases where upper limits are shown, they were derived with the help of calculations in [Ha02] or with refined versions of those calculations.

TABLE V. Relative intensities of β -delayed γ rays in the superallowed β -decay daughters. These data are used to determine some of the branching ratios presented in Table IV. (See Table VIII for the correlation between the alphabetical reference code used in this table and the actual reference numbers.)

Parent/daughter nuclei	Daughter ratios ^a	Measured γ -ray ratio		Average value	
		1	2	Ratio	Scale
¹⁸ Ne	¹⁸ F	$\gamma_{660}/\gamma_{1042}$	0.0169 ± 0.0004 [He82] 0.01733 ± 0.00012 [Gr13]	0.0172 ± 0.0005 [Ad83]	0.01729 ± 0.00011 1.0
²⁶ Si	²⁶ Al	$\gamma_{1434}/\gamma_{829}$	0.0009 ± 0.0001 [En88]	0.0015 ± 0.0006 [Be19]	0.0009 ± 0.0001 1.0
		$\gamma_{1622}/\gamma_{829}$	0.149 ± 0.016 [Mo71] 0.1245 ± 0.0023 [Wi80] 0.1322 ± 0.0016 [Be19]	0.134 ± 0.005 [Ha75] 0.1301 ± 0.0062 [Ma08]	0.1301 ± 0.0021 1.7
		$\gamma_{1655}/\gamma_{829}$	0.00145 ± 0.00032 [Wi80] 0.0017 ± 0.0007 [Be19]	0.0014 ± 0.0001 [En88]	0.0014 ± 0.0001 1.0
		$\gamma_{1843}/\gamma_{829}$	0.013 ± 0.003 [Mo71] 0.01179 ± 0.00027 [Wi80]	0.016 ± 0.003 [Ha75] 0.0130 ± 0.0007 [Be19]	0.0120 ± 0.0004 1.6
		$\gamma_{2512}/\gamma_{829}$	0.00282 ± 0.00010 [Wi80]	0.0032 ± 0.0005 [Be19]	0.0028 ± 0.0001 0.1472 ± 0.0021
		$\gamma_{\text{total}}/\gamma_{829}$			0.1472 ± 0.0021
³⁰ S	³⁰ P	$\gamma_{709}/\gamma_{677}$	0.006 ± 0.003 [Mo71]	0.0037 ± 0.0009 [Wi80]	0.0039 ± 0.0008 1.0
		$\gamma_{2341}/\gamma_{677}$	0.033 ± 0.002 [Mo71]	0.0290 ± 0.0006 [Wi80]	0.0293 ± 0.0010 1.9
		$\gamma_{3019}/\gamma_{677}$	0.00013 ± 0.00006 [Wi80]		0.00013 ± 0.00006 0.0333 ± 0.0013
		$\gamma_{\text{total}}/\gamma_{677}$			0.0333 ± 0.0013
⁴² Ti	⁴² Sc	$\gamma_{1888}/\gamma_{611}$	0.0073 ± 0.0010 [Mo15]		0.0073 ± 0.0010
⁴⁶ Cr	⁴⁶ V	$\gamma_{\text{total}}/\gamma_{993}$	0.642 ± 0.026 [Mo15]		0.642 ± 0.026
⁵⁰ Fe	⁵⁰ Mn	$\gamma_{\text{total}}/\gamma_{651}$	0.158 ± 0.015 [Mo15]		0.158 ± 0.015
⁵⁴ Ni	⁵⁴ Co	$\gamma_{\text{total}}/\gamma_{937}$	0.0576 ± 0.0043 [Mo15]		0.0576 ± 0.0043

^a γ -ray intensities are denoted by γ_E , where E is the γ -ray energy in keV. Where γ_{total} appears in the numerator, it refers to the total intensity of all known γ rays *except* the γ ray specified in the denominator.

entirely even though they have an apparently acceptable uncertainty. Those references and the reason for their exclusion from our database are listed in Table VII.

B. Data tables

The Q_{EC} -value data appear in Tables I and II. In deriving each world average Q_{EC} value—the parent-daughter atomic-mass difference—we have always focused, where possible, on direct measurements of the Q_{EC} value itself, either from reactions that connected the parent and daughter nuclei, or more recently from Penning-trap measurements that determined the parent and daughter masses in the same experiment based on

the ratio of their corresponding cyclotron frequencies. Only if such measurements were unavailable, did we resort to extracting Q_{EC} values from the difference between independent and unconnected results for the parent and daughter masses. Over the years as Penning-trap measurements have become more sophisticated, the number of cases without directly measured Q_{EC} values has steadily decreased. Now only 6 of the 23 superallowed decays listed in Table I still rely on independent mass measurements, and none of those are among the 15 best known cases.

Every direct measurement of a Q_{EC} value is identified in column 3 of Table I either by “ $Q_{\text{EC}}(\text{sa})$ ” or by “ $Q_{\text{EC}}(\text{gs})$ ” depending on whether it was the superallowed transition itself

TABLE VI. References for which the original decay-energy results have been updated to incorporate the most recent calibration standards. (See Table VIII for the correlation between the alphabetical reference code used in this table and the actual reference numbers.)

References (parent nucleus) ^a	Update procedure
Bo64 (¹⁸ Ne), Ba84 (¹⁰ C), Br94 (^{26m} Al) Ba98 (¹⁰ C), Ha98 (^{38m} K), To03 (¹⁴ O) Pr67 (¹⁸ Ne)	We have converted all original (p, n) threshold measurements to Q values using the most recent mass excesses [Wa17]. Before conversion to a Q value, this (p, n) threshold was adjusted to reflect a new value for the ⁷ Li(p, n) threshold [Wh85], which was used as calibration.
Ba88 and Ba89 (¹⁰ C)	These measurements of excitation energies in ¹⁰ B have been updated to modern γ -ray standards [He00].
Ki89 (⁴² Sc)	This ⁴¹ Ca(p, γ) reaction Q value was measured relative to that for ⁴⁰ Ca(p, γ); we have slightly revised the result based on modern mass excesses [Wa17].
Ku09 (⁴² Ti)	The result has been updated to incorporate the effect of the ⁴² Sc - ⁴² Ca Q_{EC} value from [Er17]. The change was very small.

^aThese references all appear in Table I under the appropriate parent nucleus.

TABLE VII. References from which some or all results have been rejected even though their quoted uncertainties qualified them for inclusion. (See Table VIII for the correlation between the alphabetical reference code used in this table and the actual reference numbers.)

References (parent nucleus)	Reason for rejection
1. Decay energies: Ro74 (^{10}C) Ba77b (^{10}C) Vo77 ($^{26}\text{Al}^m$, ^{34}Cl , ^{42}Sc , ^{46}V , ^{50}Mn , ^{54}Co) Wh81 and Ba98 (^{14}O) Sa09 (^{70}Br)	P. H. Barker (coauthor) later considered that inadequate attention had been paid to target surface purity [Ba84]. P. H. Barker (coauthor) later stated [Ba84] that the (p, t) reaction Q value could not be updated to incorporate modern calibration standards. Most of the results in this reference disagree significantly with more recent and accurate measurements. A detailed justification for rejection is presented in our 2009 survey [6]. The result in [Wh81] was updated in [Ba98] but then eventually withdrawn by P. H. Barker (coauthor) in [To03]. The result is inconsistent with Q_{EC} -value systematics. The full explanation appears in our 2015 survey [7].
2. Half-lives: He61 (^{14}O), Ba62 (^{14}O), Fr63 (^{14}O), Fr65 (^{42}Sc , ^{50}Mn), Si72 (^{14}O) Ha72a (^{34}Cl , ^{42}Sc) Ch84 (^{38m}K) Ia06 (^{34}Ar) Ma08 (^{26}Si)	Quoted uncertainties are too small, and results likely biased, in light of statistical difficulties more recently understood (see [Fr69a]). In particular, “maximum-likelihood” analysis was not used. All four half-lives quoted in this reference are systematically higher than more recent and accurate measurements. “Maximum-likelihood” analysis was not used. The result was withdrawn by the authors and replaced with a new result in [Ia19a]. No account was taken of the β -detection-efficiency difference between the parent and daughter activities. See [Ia10] for a more detailed explanation.
3. Branching-ratios: Ga69 (^{42}Ti)	The 2222-keV β -delayed γ ray claimed in this paper has been attributed to background [Ch16] and was not observed in a more recent measurement [Mo15].

that was directly measured or the ground-state-to-ground-state transition in cases for which one of the analog 0^+ states is an excited state. In the latter cases, the excitation energy of the analog 0^+ state is identified in column 3 by “ $E_x(\text{p}0^+)$ ” or “ $E_x(\text{d}0^+)$ ”, the “p” or “d” designating whether the excited state is in the parent or daughter nucleus. Each individual Q_{EC} and E_x result is itemized with its appropriate reference(s) in the next three columns. The weighted average of all measurements for a particular decay appears in column 7, with the corresponding scale factor (see Sec. II A) in column 8.

Note that a few of the early reaction measurements, which we updated in our previous surveys to incorporate more modern calibration data, are still precise enough to warrant their continued inclusion in Table I. These have been specified in Table VI along with a brief description of what procedure was used to update them to 2020 standards. Some other published measurements, apparently qualified for inclusion in our data base, have been withdrawn by their authors or have been rejected for well substantiated reasons. These references are identified and the reasons for rejection given in Table VII.

Five cases, ^{14}O , ^{26m}Al , ^{42}Sc , ^{50}Mn , and ^{54}Co , have a further complication: In addition to the individual Q_{EC} -value results, Q_{EC} -value differences have also been obtained via ($^3\text{He}, t$) reactions on composite targets. These difference measure-

ments are presented in Table II. They have been dealt with in combination with the direct Q_{EC} -value measurements to obtain a best overall fit by a method described in Sec. II A. The final average Q_{EC} value for each transition appears in column 7 of Table I and the average differences are in column 4 of Table II. All are flagged with footnotes to indicate the interconnection.

For the six transitions without direct Q_{EC} -value measurements, the measured mass excesses of the parent and daughter nuclei are designated by ME(p) and ME(d), respectively, and the Q_{EC} value that appears in column 7 of Table I is simply derived from the difference between the two average mass excesses.

In all 23 cases, the final average Q_{EC} value for the superallowed transition appears in column 7 in bold print.

Half-life data are presented in Table III, where the format is similar to that of Table I. Unlike the Q_{EC} results, half-life measurements cannot be updated without access to the primary data. A number of mostly pre-1970 measurements claimed very tight error bars but nonetheless have had to be rejected because they were not analyzed with the “maximum-likelihood” fitting procedure. The importance of using this technique for precision half-life measurements was not recognized until 1969 [73]. Data acquired over half a century ago cannot be reconstituted and reanalyzed, so we have rejected

TABLE VIII. Reference key relating alphabetical reference codes used in Tables I–VII to the actual reference numbers.

Table code	Reference number	Table code	Reference number	Table code	Reference number	Table code	Reference number	Table code	Reference number	Table code	Reference number
Ad83	[8]	Aj88	[9]	Aj91	[10]	Al72	[11]	Al75	[12]	Al77	[13]
Al78	[14]	Al82	[15]	Az74	[16]	Az75	[17]	Ba62	[18]	Ba77a	[19]
Ba77b	[20]	Ba84	[21]	Ba88	[22]	Ba89	[23]	Ba90	[24]	Ba98	[25]
Ba00	[26]	Ba01	[27]	Ba04	[28]	Ba06	[29]	Ba09	[30]	Ba10	[31]
Be77	[32]	Be78	[33]	Be85	[34]	Be08	[35]	Be19	[36]	Bl04a	[37]
Bl04b	[38]	Bl10	[39]	Bl15	[40]	Bo64	[41]	Br94	[42]	Bu88	[43]
Bu06	[44]	Ca05	[45]	Ch84	[46]	Ch13	[47]	Ch16	[48]	Cl73	[49]
Da80	[50]	Da85	[51]	De69	[52]	De78	[53]	Dr75	[54]	Du13	[55]
Du16	[56]	Du17	[57]	En88	[58]	Er06a	[59]	Er06b	[60]	Er08	[61]
Er09a	[62]	Er09b	[63]	Er11	[64]	Er17	[65]	Et11	[66]	Fa09	[67]
Fi08	[68]	Fi11	[69]	Fi12	[70]	Fr63	[71]	Fr65	[72]	Fr69a	[73]
Fr75	[74]	Fu99	[75]	Ga69	[76]	Ga01	[77]	Ge08	[78]	Go72	[79]
Gr00	[80]	Gr08	[81]	Gr13	[82]	Ha72a	[83]	Ha74a	[84]	Ha74b	[85]
Ha74d	[86]	Ha75	[87]	Ha94	[88]	Ha98	[89]	Ha02	[90]	Ha03	[91]
He61	[92]	He81	[93]	He82	[94]	He00	[95]	He02	[96]	Ho64	[97]
Ho74	[98]	Hu82	[99]	Hy03	[100]	Hy05	[101]	Ia06	[102]	Ia08	[103]
Ia10	[104]	Ia18	[105]	Ia19a	[106]	Ia19b	[107]	In77	[108]	Is80	[109]
Ji02	[110]	Ka69	[111]	Ke07	[112]	Ki89	[113]	Ki91	[114]	Ko83	[115]
Ko87	[116]	Ko97a	[117]	Ko97b	[118]	Kr91	[119]	Ku09	[120]	Kw13	[121]
La13	[122]	La15	[123]	Le08	[124]	Li94	[125]	Ma94	[126]	Ma08	[127]
Mo71	[128]	Mo15	[129]	Mo17	[130]	Mu04	[131]	Na91	[132]	Oi01	[133]
On05	[134]	Pa11	[135]	Pa12	[136]	Pa14	[137]	Pa15	[138]	Pi03	[139]
Pr67	[140]	Pr90	[141]	Ra83	[142]	Re99	[143]	Re17	[144]	Ro72	[145]
Ro74	[146]	Ro75	[147]	Ro06	[148]	Ry73	[149]	Sa80	[150]	Sa95	[151]
Sa04	[152]	Sa05	[153]	Sa09	[154]	Sc07	[155]	Sc11	[156]	Se73	[157]
Si66	[158]	Si72	[159]	So11	[160]	Sq75	[161]	Ta12	[162]	To03	[163]
To05	[164]	Tr77	[165]	Va15	[166]	Vo77	[167]	Vo15	[168]	Wa67	[169]
Wa83	[170]	Wa92	[171]	Wa17	[172]	Wh81	[173]	Wh85	[174]	Wi76	[175]
Wi78	[176]	Wi80	[177]	Zh17	[178]	Zh18	[179]	Zi72	[180]	Zi87	[181]

these measurements. They are documented in Table VII together with several half-life measurements that were rejected for other reasons.

Finally, the branching-ratio measurements appear in Table IV. There the decays of the $T_z = -1$ and $T_z = 0$ parents are seen to be quite different from one another. The former generally feature several strong Gamow-Teller branches that compete with the superallowed (Fermi) transition, while the latter are overwhelmingly dominated by the superallowed transition. This is because the $T_z = -1$ parents populate odd-odd daughters, which offer a number of energetically accessible 1^+ states, while the $T_z = 0$ parents decay to even-even daughters, which are without low-lying 1^+ states.

The $T_z = 0$ parents are the most straightforward to deal with since, in all cases, the superallowed branch accounts for $> 99.5\%$ of the total decay strength. Thus, even imprecise measurements of the weak nonsuperallowed branches can be subtracted from 100% to yield the superallowed branching ratio with good relative precision. However, there is an important feature to be taken account of for the higher- Z parents of this type, because their Q_{EC} values are large enough that relatively high-lying 1^+ states in their daughters become accessible to β decay. It has been shown theoretically [90] and experimentally (see Refs. [68] for ^{62}Ga and [55,139] for ^{74}Rb)

that numerous very weak Gamow-Teller transitions occur, which, in total, can carry significant decay strength—the Pandemonium effect [183]. Where such unobserved transitions are expected to exist but have not already been accounted for in the quoted references, we have used a combination of experiment and theory to arrive at an upper limit for the unobserved strength, with uncertainties being adjusted accordingly. All such cases are flagged with a footnote in the table.

The branching ratios for decays from $T_z = -1$ parents are much more experimentally challenging to determine, since the superallowed branch is usually one of several comparably strong branches—with the notable exception of ^{14}O —and, in two of the measured cases, the superallowed branching ratio is actually less than 10%. Not only that, but in most of these cases the superallowed β branch is not followed by a prompt decay γ ray in the daughter. Since it is only from the intensities of β -delayed γ rays that the β -branching ratios can be determined experimentally, these superallowed branching ratios must be determined in three steps: First, the absolute branching of the strongest Gamow-Teller branch is determined from the intensity of its subsequent prompt γ -decay peak; then the intensities of the other nonsuperallowed transitions are established from the full spectrum of γ -ray

TABLE IX. Derived ft values for superallowed Fermi β decays.

Parent nucleus	f	P_{EC} (%)	Partial half-life t (ms)	ft (s)
$T_z = -1$				
^{10}C	2.30169 ± 0.00070	0.297	1321800 ± 1800	3042.4 ± 4.1
^{14}O	42.8031 ± 0.0077	0.088	71075 ± 15	3042.23 ± 0.84
^{18}Ne	134.64 ± 0.17	0.081	21630 ± 590	2912 ± 79
^{22}Mg	418.35 ± 0.13	0.069	7293 ± 16	3051.1 ± 6.9
^{26}Si	1028.03 ± 0.12	0.064	2969.0 ± 5.4	3052.2 ± 5.6
^{30}S	1977.32 ± 0.39	0.065	1525 ± 20	3015 ± 41
^{34}Ar	3410.85 ± 0.25	0.069	896.55 ± 0.81	3058.0 ± 2.8
^{38}Ca	5328.88 ± 0.31	0.075	574.8 ± 1.1	3062.8 ± 6.0
^{42}Ti	7130.1 ± 1.4	0.087	433 ± 12	3090 ± 88
^{46}Cr	10685 ± 74	0.092	292.6 ± 9.1	3126 ± 100
^{50}Fe	15060 ± 60	0.100	205.8 ± 4.7	3099 ± 71
^{54}Ni	21137 ± 57	0.104	144.9 ± 2.3	3062 ± 50
$T_z = 0$				
^{26m}Al	478.270 ± 0.098	0.082	$6351.24^{+0.55}_{-0.54}$	3037.61 ± 0.67
^{34}Cl	1996.003 ± 0.096	0.080	$1527.77^{+0.47}_{-0.44}$	$3049.43^{+0.95}_{-0.88}$
^{38m}K	3297.39 ± 0.15	0.085	925.42 ± 0.28	3051.45 ± 0.92
^{42}Sc	4472.46 ± 0.46	0.099	681.44 ± 0.26	3047.7 ± 1.2
^{46}V	7209.25 ± 0.54	0.101	$423.114^{+0.068}_{-0.053}$	$3050.33^{+0.54}_{-0.44}$
^{50}Mn	10745.99 ± 0.49	0.107	283.68 ± 0.11	3048.4 ± 1.2
^{54}Co	15766.8 ± 2.7	0.111	$193.495^{+0.086}_{-0.063}$	$3050.8^{+1.4}_{-1.1}$
^{62}Ga	26400.3 ± 8.3	0.137	116.441 ± 0.042	3074.1 ± 1.5
^{66}As	32119 ± 460	0.155		
^{70}Br	38600 ± 3600	0.175		
^{74}Rb	47281 ± 93	0.194	65.201 ± 0.047	3082.8 ± 6.5

peaks; and finally the total of all these β branching ratios is subtracted from 100% to yield the superallowed branching ratio.

Recent precision measurements of the decays of ^{26}Si [36], ^{34}Ar [107], and ^{38}Ca [138] have followed the full procedure and have also averaged in the relative β -delayed γ -ray intensities from other independent measurements in the literature. These results appear unaltered in Table IV. However, some older measurements determined the intensity of the strongest Gamow-Teller transitions but were insensitive to the weaker ones. Their original results for the superallowed branches had to be updated to account for transitions more recently observed. For these cases, the relevant γ -ray intensity measurements appear in Table V, with their averages then being used to determine the corresponding superallowed branching-ratio averages shown in bold type in Table IV. These cases are flagged with a footnote in the latter table.

C. The ft values

With the input data now settled, we can proceed to derive the ft values for the 23 superallowed transitions included in the tables. We calculate the statistical rate function f using the same code as in our previous survey [7]. The basic methodology for the calculation is described in the Appendix to our 2004 survey [5], with refinements applied to incorporate excitation of the daughter atom, as explained in Appendix A of our 2008 survey [6]. Our final f values

for the $T = 1$ transitions of interest here are recorded in the second column of Table IX. They were evaluated with the Q_{EC} values and their uncertainties taken from column 7 of Table I.

The third column of Table IX lists (as percentages) the electron-capture fraction, P_{EC} , calculated for each of the 23 superallowed transitions. The method of calculation was described in our 2004 survey [5], to which the reader is referred for more details. The partial half-life, t , for each transition is then obtained from its total half-life, $t_{1/2}$, branching ratio, R , and electron-capture fraction according to the following formula:

$$t = \frac{t_{1/2}}{R}(1 + P_{EC}). \quad (7)$$

The resultant values for the partial half-lives and the corresponding ft values appear in columns 4 and 5 of the table.

These tabulated ft values may be regarded as unambiguously experimental results. To proceed further, though, to the corresponding $\mathcal{F}t$ values we require the intervention of theory. As laid out in Eq. (1), it is necessary to apply the small transition-dependent correction terms, δ'_R , δ_{NS} , and δ_C to an ft value in order to obtain $\mathcal{F}t$. Moreover, the transition-independent radiative correction Δ_R^V is required to advance beyond the $\mathcal{F}t$ values to derive a value for G_V and open up more general tests of weak-interaction physics.

These four theoretical correction terms are described in more detail in the following section.

III. THEORETICAL CORRECTIONS

A. Radiative corrections

A measured β -decay half-life includes both bare-decay and radiative-decay processes, such as bremsstrahlung. Since it is the half-life of the bare-decay process that is required for the $\mathcal{F}t$ value, the measured ft result has to be amended with a radiative-correction calculation. It is convenient to break down this correction, RC, into components

$$\text{RC} = \Delta_R^V + \delta'_R + \delta_{\text{NS}}. \quad (8)$$

Of these components, Δ_R^V is independent of the particular transition involved, δ'_R is weakly dependent on it and δ_{NS} is strongly dependent. The principal contributing graphs are the one-photon bremsstrahlung, the γW -box and ZW -box diagrams. These box diagrams contain loop integrations. It has been computationally convenient to separate the low-energy part of the integration from the high-energy part and to make different assumptions in the two energy regimes. We will deal with the correction terms one by one.

1. The Δ_R^V radiative correction

The Δ_R^V correction is universal: the same for both neutron and all superallowed nuclear β decays. It is computed from the loop graphs. In particular, in the γW -box diagram the weak-interaction hadron vertex can be either vector like, accompanied by an isovector hadron electromagnetic vertex, or axial-vector like, accompanied by an isoscalar electromagnetic vertex. Only these two combinations preserve G parity at the hadron vertices.

In their original evaluation of this correction Marciano and Sirlin [184,185] wrote the correction as

$$\Delta_R^V = \frac{\alpha}{2\pi} \left[3 \ln \frac{m_W}{m_p} + \ln \frac{m_W}{m_A} + 2C_{\text{Born}} - 4 \ln \frac{m_W}{m_Z} + \mathcal{A}_g \right], \quad (9)$$

where m_p , m_W , and m_Z are the masses of the proton, W boson, and Z boson, respectively. The first term in this expression is from the vector interaction in the γW -box diagram; the second and third are from the axial-vector interaction; the fourth term is from the ZW -box diagram; and the fifth is a small QCD correction, $\mathcal{A}_g \simeq 0.34$. The first term is protected by the CVC hypothesis and is free of strong-interaction QCD contaminations. That is not true of the axial-vector contributions, which, although small, contain most of the theoretical uncertainty coming from the strong interaction effects. In Eq. (9), $C_{\text{Born}} \simeq 0.86$ is the Born (elastic) amplitude contribution, and $m_A \simeq 1.2$ GeV is a hadronic short-distance cut-off employed by Marciano and Sirlin [184,185] to separate the low-energy and high-energy regimes.

In 2006, the same authors revised their procedure [186] by introducing an interpolation function between the low-energy and high-energy regions. This gave a better control over the assigned uncertainties but did not change the central value of Δ_R^V very much. Their result, $\Delta_R^V = (2.361 \pm 0.038)\%$ appears

TABLE X. Recent values of the nucleus-independent radiative correction Δ_R^V in percentage units, and our adopted value.

Reference	Δ_R^V (%)
Marciano and Sirlin [186] 2006	2.361 ± 0.038
Seng <i>et al.</i> [187,188] 2018/19	2.467 ± 0.022
Czarnecki, Marciano and Sirlin [189] 2019	2.426 ± 0.032
Adopted value	2.454 ± 0.019

in the top line of Table X. It became the adopted standard for the next decade and was used by us in subsequent surveys. Only recently has the issue been reopened.

Seng, Gorchtein, Patel, and Ramsey-Musolf [187,188] began their reassessment by expressing the γW -box contribution to Δ_R^V in terms of a dispersion relation, which relates its axial-vector contribution directly to measurable inclusive lepton-hadron and neutrino-hadron structure functions. Using existing data on neutrino and antineutrino scattering, they obtained a more precise, but significantly larger, value for Δ_R^V of $(2.467 \pm 0.022)\%$. It also appears on the second line of Table X. As explained later (see Sec. VA), this increase in Δ_R^V has a consequential impact on the CKM-matrix unitarity test. A larger Δ_R^V leads to a lower value for the deduced CKM matrix element, V_{ud} , and sets up tension in meeting the unitarity sum rule for the top-row elements of that matrix.

With that important impact as motivation, Czarnecki, Marciano, and Sirlin [189] revisited their own work, improving their use of the Bjorken sum rule to constrain the strong-interaction corrections to the axial-vector component of the γW -box diagram. Their new result for Δ_R^V is $(2.426 \pm 0.032)\%$, which can be seen from Table X to lie between their original value and the dispersion-relation result. On the bottom line of the table we present our adopted value,

$$\Delta_R^V = (2.454 \pm 0.019)\%, \quad (10)$$

which is a weighted average—as per Eqs. (3) and (4)—of the two most recent results. A scale factor of $S = 1.06$ has been applied to its uncertainty.

2. The δ'_R radiative correction

The δ'_R correction is principally a QED calculation depending only on the charge Z of the nucleus involved and the maximum energy, E_m , of the emitted electron. The correction comes from the bremsstrahlung and the low-energy part of the γW -box diagram. These diagrams have to be considered together because collectively they remove the divergence in the box graph as the photon energy goes to zero. We write δ'_R as

$$\delta'_R = \frac{\alpha}{2\pi} [\bar{g}(E_m) + \delta_2 + \delta_3 + \delta_{\alpha^2}]. \quad (11)$$

The function $\bar{g}(E_m)$ is an average over the β -decay spectrum of the function $g(E, E_m)$, which is defined by Sirlin in Eq. (20b) of Ref. [185]. The next two terms, δ_2 and δ_3 , represent corrections to order $Z\alpha^2$ and $Z^2\alpha^3$, respectively, in which the electron interacts with the Coulomb field of the nucleus. Care is taken not to double count with the Fermi function. The calculations to date [190,191] are complete to order $Z\alpha^2$ but

only estimated by the leading log term in order $Z^2\alpha^3$. Last, δ_{α^2} , is an order- α^2 correction that is quite small and is discussed in Ref. [192].

We list the values of all five individual terms in Table V of Ref. [192] for all but the three transitions from ^{46}Cr , ^{50}Fe , and ^{54}Ni ; their values appear in Table VII of Ref. [193]. The resulting totals, δ'_R , for all transitions are given here in Table XVI, which appears in Sec. IV. They are given without uncertainties since, as in our 2015 survey [7], we treat the uncertainty in δ'_R as being systematic. This will be discussed in more detail in Sec. IV.

3. The δ_{NS} radiative correction

In Sec. III A 1, the Eq. (9) expression for the universal correction Δ_R^V includes the Born elastic contribution to the low-energy part of the γW -box diagram, which comes from axial-vector weak couplings and isoscalar electromagnetic couplings:

$$C_{\text{Born}} \simeq 0.77g_A g_S^{(0)} \simeq 0.86, \quad (12)$$

where 0.77 is an estimate of the loop integration, $g_A \simeq 1.27$ is the axial-vector coupling constant, and $g_S^{(0)} = 0.88$ is the isoscalar-spin-magnetic-moment coupling. This result, however, is calculated for a free neutron and could be modified when the neutron is embedded in the nucleus.

Thus, we rewrite C_{Born} as the sum of two terms:

$$C_{\text{Born}} \rightarrow C_{\text{Born}}^{\text{free}} + C_{\text{NS}}, \quad (13)$$

where $C_{\text{Born}}^{\text{free}}$ is retained in Δ_R^V , and a nuclear-structure dependent part, C_{NS} , is separated out into a separate radiative-correction term δ_{NS} . This term is itself split into two parts:

$$\delta_{\text{NS}} = \frac{\alpha}{\pi} C_{\text{NS}} = \delta_{\text{NS},A} + \delta_{\text{NS},B}. \quad (14)$$

The first part, $\delta_{\text{NS},A}$, arises from the observation that axial-vector couplings and spin-magnetic-moment couplings are quenched in nuclei, so that $g_A \rightarrow q_A g_A$ and $g_S^{(0)} \rightarrow q_S^{(0)} g_S^{(0)}$, where q_A and $q_S^{(0)}$ are quenching factors. Towner [194] estimated these quenching factors to give

$$\delta_{\text{NS},A} = \frac{\alpha}{\pi} [q_A q_S^{(0)} - 1] C_{\text{Born}}^{\text{free}}. \quad (15)$$

The second part of the structure-dependent term, $\delta_{\text{NS},B}$, arises because the weak interaction and isoscalar electromagnetic interaction may not be with the same nucleon in the nucleus. This was first pointed out by Jaus and Rasche [195] and implemented by Towner [196] in a nuclear shell-model calculation. The results for $\delta_{\text{NS},A}$ and $\delta_{\text{NS},B}$ are given in columns two and three of Table XI.

Recently, Seng, Gorchtein, and Ramsey-Musolf [188] have suggested that the assumptions made by Towner [194] to calculate $\delta_{\text{NS},A}$ may not be well founded. One of their criticisms is that the quenching factors q_A and $q_S^{(0)}$ obtained from experimental Gamow-Teller β transitions and electromagnetic gamma transitions are not necessarily the quenching factors required when the weak and electromagnetic vertices are part of the γW -box diagram. Another, is that only low-energy intermediate states are in play when, in principle, the full

nuclear Green's function should be in use, especially the contributions from the quasielastic region.

These authors propose an alternative method of addressing the modification of the free-nucleon Born contribution based on a quasielastic single-nucleon knockout process. They use a Fermi gas model to give a numerical estimate of the effect, arriving at an average result of

$$\delta_{\text{NS},A} = \frac{\alpha}{\pi} [-0.47 \pm 0.14] = -0.109(33)\%. \quad (16)$$

The only nucleus-dependent part of this calculation is the removal energy for the nucleon in the knockout process. Since this removal energy does not differ much from nucleus to nucleus for the cases under study, its range of values is incorporated into the error estimate. This result is about a factor of two larger than Towner's results given in column two of Table X, which do not change much either from nucleus to nucleus and yield a similarly derived average value of $-0.057(10)\%$.

Yet a further small contribution to δ_{NS} has been identified by Gorchtein [197]. He argues that nuclear polarizabilities cause a distortion to the emitted-electron energy spectrum and that this effect has not been considered before. Being linearly dependent on the electron energy, this correction term might appropriately be included in δ'_R . However, since the calculational method used by Gorchtein is very similar to that of Seng *et al.* [188], we choose to keep it within δ_{NS} and designate it as $\delta_{\text{NS},E}$.

Gorchtein [197] estimated this correction in two ways. First, from dimensional analysis with the photonuclear sum rule, he obtained $\delta_{\text{NS}}(E) = 0.004 E \%$, with E being the electron energy in MeV. Second, from the free Fermi-gas model, he obtained $\delta_{\text{NS}}(E) = (0.028 \pm 0.004) E \%$. The Fermi-gas model is known to overestimate the quasielastic response at low energies so it is not surprising that the latter estimate is an order-of-magnitude larger than the naive estimate. Thus, Gorchtein considered it appropriate to take the average of these two results and assign a 100% error, obtaining

$$\delta_{\text{NS}}(E) = (0.016 \pm 0.016) E \%. \quad (17)$$

To convert this result into the form required to correct the superallowed ft values, $\delta_{\text{NS}}(E)$ has to be integrated over the electron spectrum for each transition. Because the average value of E is approximately $Q_{\text{EC}}/2$, the correction becomes

$$\delta_{\text{NS},E} = \langle \delta_{\text{NS}}(E) \rangle = (0.008 \pm 0.008) Q_{\text{EC}} \%, \quad (18)$$

where the Q_{EC} value is expressed in MeV.

In conclusion, our adopted value for the δ_{NS} radiative correction is

$$\delta_{\text{NS}} = \delta_{\text{NS},A} + \delta_{\text{NS},B} + \delta_{\text{NS},E}, \quad (19)$$

where for $\delta_{\text{NS},A}$ we use the new result from Ref. [188], which appears in Eq. (16), to replace the earlier Towner [194] values, which are listed in the second column of Table XI and were based on simple quenching ideas. For $\delta_{\text{NS},B}$ we continue to use the results from Ref. [196]; they appear in column three of Table XI. The $\delta_{\text{NS},E}$ values we use are from Gorchtein's work [197], as expressed in Eq. (18) and listed in column four

TABLE XI. Component contributions to the radiative correction, δ_{NS} in percentage units. The last column gives our adopted value with first a statistical error and then a systematic error.

Parent Nucleus	Towner ^a		Gorchtein ^b	Adopted ^c
	$\delta_{\text{NS},A}(\%)$	$\delta_{\text{NS},B}(\%)$	$\delta_{\text{NS},E}(\%)$	$\delta_{\text{NS}}(\%)$
$T_z = -1$				
¹⁰ C	-0.041(4)	-0.306(35)	0.015(15)	-0.400(35)(36)
¹⁴ O	-0.048(5)	-0.196(50)	0.023(23)	-0.283(50)(40)
¹⁸ Ne	-0.046(5)	-0.244(35)	0.027(27)	-0.326(35)(42)
²² Mg	-0.049(5)	-0.174(19)	0.033(33)	-0.250(19)(46)
²⁶ Si	-0.053(5)	-0.164(19)	0.039(39)	-0.234(19)(51)
³⁰ S	-0.056(6)	-0.129(14)	0.044(44)	-0.195(14)(54)
³⁴ Ar	-0.060(6)	-0.121(14)	0.049(49)	-0.181(14)(58)
³⁸ Ca	-0.063(6)	-0.110(14)	0.053(53)	-0.167(14)(62)
⁴² Ti	-0.056(6)	-0.180(19)	0.056(56)	-0.233(19)(65)
⁴⁶ Cr	-0.058(6)	-0.116(19)	0.061(61)	-0.164(19)(69)
⁵⁰ Fe	-0.059(6)	-0.096(19)	0.065(65)	-0.140(19)(73)
⁵⁴ Ni	-0.061(6)	-0.104(19)	0.070(70)	-0.143(19)(77)
$T_z = 0$				
^{26m} Al	-0.053(5)	+0.056(19)	0.034(34)	-0.019(19)(47)
³⁴ Cl	-0.060(6)	-0.027(14)	0.044(44)	-0.093(14)(55)
^{38m} K	-0.063(6)	-0.037(14)	0.048(48)	-0.098(14)(58)
⁴² Sc	-0.056(6)	+0.091(19)	0.051(51)	+0.033(19)(61)
⁴⁶ V	-0.058(6)	+0.022(8)	0.056(56)	-0.031(8)(65)
⁵⁰ Mn	-0.059(6)	+0.020(8)	0.061(61)	-0.029(8)(69)
⁵⁴ Co	-0.061(6)	+0.026(8)	0.066(66)	-0.017(8)(74)
⁶² Ga	-0.063(6)	+0.020(19)	0.073(73)	-0.016(19)(80)
⁶⁶ As	-0.065(6)	+0.002(19)	0.077(77)	-0.030(19)(83)
⁷⁰ Br	-0.066(7)	-0.020(24)	0.080(80)	-0.049(24)(86)
⁷⁴ Rb	-0.067(7)	-0.006(29)	0.083(83)	-0.032(29)(89)

^aReference [194,196].^bReference [197].^cThe sum of $\delta_{\text{NS},A}$ from Eq. (16) with $\delta_{\text{NS},B}$ from column 3 and $\delta_{\text{NS},E}$ from column 4 of this table.

of Table XI. Our adopted values for the total δ_{NS} are in column five. Two uncertainties are cited. The first is from $\delta_{\text{NS},B}$, which is specific to the nucleus under study, so we treat it as a statistical uncertainty. The second is from $\delta_{\text{NS},A}$ in Eq. (16) and from $\delta_{\text{NS},E}$ in Eq. (18), which we combine in quadrature. Since this uncertainty is nucleus-independent, we will treat it as being systematic.

B. Isospin symmetry breaking corrections δ_C

1. CVC filter for δ_C corrections

As specified in Eq. (1), the isospin-symmetry-breaking correction, δ_C , is one of several corrections applied to experimentally determined $0^+ \rightarrow 0^+ ft$ values to produce corrected $\mathcal{F}t$ values, which, according to the conservation of vector current (CVC), should all have the same value independent of the nucleus under study. We harnessed this thought in 2010 by proposing [198] that a CVC test be used to discriminate between various sets of δ_C calculations available in the literature: If CVC expectations were not met and a set of calculations did not lead to statistically consistent $\mathcal{F}t$ values, then the δ_C calculations were rejected. We followed this prescription in our most recent survey [7] with the conclusion that only one set

then available—denoted SM-WS and taken from Ref. [192]—met the required standard.

Since that last survey, there has been further work on δ_C by Satula *et al.* [199] using density functional theory (DFT). Briefly, they start with a self-consistent Slater-determinant state obtained from a solution of the axially deformed Skyrme-Hartree-Fock equations. That state violates both rotational and isospin symmetries, so their strategy is to restore rotational invariance and remove spurious isospin mixing by a re-diagonalization of the Hamiltonian in a basis that conserves these quantities. In their original work [200], an unacceptably large correction, $\delta_C \simeq 10\%$, was obtained for $A = 38$, a consequence of the calculation shifting the energy of the $2s_{1/2}$ subshell too close to the Fermi surface. In their more recent work [199] they invoke a new variant of the no-core-configuration interaction model while still treating properly the isospin and rotational symmetries. Their new result for $A = 38$ is $\delta_C = 1.7\%$, down considerably from their previous 10% result, but still a factor of two larger than the semiphenomenological result from the SM-WS calculation.

In Table XII, we list the δ_C values from the DFT model of Satula *et al.* [199] and compare them with the semiphenomenological calculations, SM-WS, of Towner and Hardy [192]. Note that the DFT calculations only cover a subset of

TABLE XII. DFT calculation of the isospin-symmetry-breaking correction δ_C from Ref. [199] compared with the results from the semiphenomenological SM-WS calculation given in Table XIV.

Parent nucleus	DFT δ_C (%)	SM-WS δ_C (%)
$T_z = -1$		
^{10}C	0.58(9)	0.18(2)
^{14}O	0.30(3)	0.33(3)
^{22}Mg	0.27(4)	0.39(2)
^{34}Ar	0.87(13)	0.66(4)
$T_z = 0$		
^{26m}Al	0.33(5)	0.31(2)
^{34}Cl	0.75(11)	0.61(5)
^{42}Sc	0.77(27)	0.69(5)
^{46}V	0.56(8)	0.62(6)
^{50}Mn	0.48(7)	0.66(3)
^{54}Co	0.59(9)	0.77(7)
^{62}Ga	0.78(12)	1.48(21)
^{74}Rb	1.63(24)	1.62(27)
χ^2/ν	8.1 ^a	1.2

^aThe result for ^{62}Ga has not been included in the least-squares fit from which this value for χ^2/ν has been obtained.

the transitions we have been surveying here. We performed the CVC-consistency test exactly as we did for Table XI in Ref. [7], with the calculated δ_C uncertainties all set to zero. The resultant values for χ^2/ν appear in the last row of the table, where it is evident that the newer DFT results are still unsatisfactory in detail and thus cannot be used in our further tests of weak-interaction physics from superallowed β decay. Nevertheless, these are first-principles calculations and they play a very important role in confirming that the semiphenomenological results obtained with models such as SM-WS are not inconsistent with the broad features of such a first-principles calculation, as can be seen from a comparison of the two sets of results in Table XII.

We turn now to the semiphenomenological calculation of δ_C , where it has historically been convenient to divide the correction into two components,

$$\delta_C = \delta_{C1} + \delta_{C2}. \quad (20)$$

For δ_{C1} , a modest shell-model space (usually one major oscillator shell) is employed, in which Coulomb and other charge-dependent terms are added to the charge-independent effective Hamiltonian customarily used in the shell model. These charge-dependent additional terms are adjusted on a case-by-case basis to reproduce the coefficients of the isobaric mass multiplet equation [192].

It is recognized that the Coulomb force is long range and its influence reaches much further than the one major oscillator shell that is included in the calculation of δ_{C1} . Its principal impact is to change the structure of the proton radial function so that its shape differs slightly from its isospin-partner neutron radial function. To account for this, the term δ_{C2} is introduced to quantify this radial difference. In the Towner-Hardy model [192] the radial functions themselves are derived from a phenomenological Woods-Saxon potential. There is

TABLE XIII. The isospin-symmetry-breaking correction δ_{C2} in percentage units from Xayavong-Smirnova [201] calculations labeled BM_m -IIG and SMV-IIG and the Towner-Hardy [192] calculation labeled SM-WS. In the last column, we give an adopted value being the average of the three calculations shown.

Parent Nucleus	δ_{C2} (%) BM_m -IIG	δ_{C2} (%) SWV-IIG	δ_{C2} (%) SM-WS	Adopted δ_{C2} (%)
$T_z = -1$				
^{22}Mg	0.253(17)	0.268(21)	0.375(15) ^a	
^{26}Si	0.345(21)	0.374(18)	0.405(25)	
^{30}S	0.637(21)	0.616(25)	0.700(20)	0.651(42)
^{34}Ar	0.636(11)	0.587(18)	0.665(55) ^a	0.629(39)
^{38}Ca	0.761(39)	0.670(36)	0.745(70)	0.725(46)
$T_z = 0$				
^{26m}Al	0.245(9)	0.219(13)	0.280(15)	
^{34}Cl	0.536(25)	0.454(22)	0.550(45)	0.513(48)
^{38m}K	0.538(8)	0.465(12)	0.565(50) ^a	0.523(50)

^aValues updated from new data on nuclear rms radii [202].

a case-by-case adjustment in the Woods-Saxon potential to ensure the nuclear charge radius and the proton and neutron separation energies are correctly reproduced.

Since our last survey, there has been new work along these lines by Xayavong and Smirnova [201]. This follows closely the Towner-Hardy model [192] in using Woods-Saxon potentials, but they introduce a number of important computational improvements, especially in regards to how the fits to the nuclear charge radii are implemented. They only study eight superallowed transitions in the sd shell but investigate several different variants of the Woods-Saxon potential. They subjected all their δ_{C2} calculations to the CVC test, and only two sets, denoted RM_m -IIG and SMV-IIG, passed the test.

In Table XIII we list these two Xayavong-Smirnova [201] values along side the older Towner-Hardy [192] results. The correspondence between the two works is excellent. For our subsequent analysis we adopt for these sd -shell nuclei δ_{C2} values that are an average of the three calculations with uncertainties that span the range of the calculations. We exclude ^{22}Mg , ^{26}Si , and ^{26m}Al from this procedure because the Towner-Hardy calculation [192] in these cases goes beyond simple sd -shell configurations to include some core excitations from the p shell. This extension gives an important improvement as discussed in Ref. [192].

The full list of δ_{C1} , δ_{C2} , and total δ_C values that we use in the derivation of $\mathcal{F}t$ values for the transitions of interest appears in Table XIV. Most of the values are the same as those we used in our last survey [7], augmented by those for the transitions from ^{46}Cr , ^{50}Fe , and ^{54}Ni , which first appeared in Ref. [193]. Naturally the δ_{C2} values in column 5 of Table XIII are entered where they apply.

2. Mirror test for δ_C corrections

There is another test available, which can be applied to the calculated correction terms. It is based on the measured differences in ft values between mirror superallowed transitions: for example, $^{38}\text{Ca} \rightarrow ^{38m}\text{K}$ and $^{38m}\text{K} \rightarrow ^{38}\text{Ar}$. The method was originally proposed for that mirror pair [137] as

TABLE XIV. Corrections δ_{C1} , δ_{C2} , and δ_C that are used in the conversion of experimental ft values to fully corrected $\mathcal{F}t$ values.

Parent nucleus	δ_{C1} (%)	δ_{C2} (%)	δ_C (%)
$T_z = -1$			
^{10}C	0.010(10)	0.165(15)	0.175(18)
^{14}O	0.055(20)	0.275(15)	0.330(25)
^{18}Ne	0.155(30)	0.405(25)	0.560(39)
^{22}Mg	0.010(10)	0.375(15)	0.385(18)
^{26}Si	0.030(10)	0.405(25)	0.435(27)
^{30}S	0.155(20)	0.651(42)	0.806(46)
^{34}Ar	0.030(10)	0.629(39)	0.659(40)
^{38}Ca	0.020(10)	0.725(46)	0.745(47)
^{42}Ti	0.105(20)	0.855(60)	0.960(63)
^{46}Cr	0.045(20)	0.715(85)	0.760(87)
^{50}Fe	0.025(20)	0.635(45)	0.660(49)
^{54}Ni	0.065(30)	0.725(60)	0.790(67)
$T_z = 0$			
^{26m}Al	0.030(10)	0.280(15)	0.310(18)
^{34}Cl	0.100(10)	0.513(48)	0.613(49)
^{38m}K	0.105(20)	0.523(50)	0.628(54)
^{42}Sc	0.020(10)	0.670(45)	0.690(46)
^{46}V	0.075(30)	0.545(55)	0.620(63)
^{50}Mn	0.030(20)	0.630(25)	0.660(32)
^{54}Co	0.050(30)	0.720(60)	0.770(67)
^{62}Ga	0.275(55)	1.20(20)	1.48(21)
^{66}As	0.195(45)	1.35(40)	1.55(40)
^{70}Br	0.445(40)	1.25(25)	1.70(25)
^{74}Rb	0.115(60)	1.50(26)	1.62(27)

a method to distinguish among the different models used to calculate δ_C , but it is also useful as a test of δ_{NS} . Two more mirror pairs, $^{26}\text{Si} \rightarrow ^{26m}\text{Al}$ and $^{26m}\text{Al} \rightarrow ^{26}\text{Mg}$, as well as $^{34}\text{Ar} \rightarrow ^{34}\text{Cl}$ and $^{34}\text{Cl} \rightarrow ^{34}\text{S}$, have been completed with high precision since our last survey so the strength of the test has been considerably increased.

Like the δ_C filter described in the last section, this test is based on the CVC premise that the corrected $\mathcal{F}t$ values defined in Eq. (1) must be nucleus independent. In that case, the ratio of ft values for a pair of mirror transitions can be written as

$$\frac{ft^a}{ft^b} = 1 + (\delta_R^b - \delta_R^a) + (\delta_{NS}^b - \delta_{NS}^a) - (\delta_C^b - \delta_C^a), \quad (21)$$

TABLE XV. Calculated differences in δ_R^b , δ_{NS} , and δ_C for seven mirror doublets expressed in percent units, and the resultant ft^a/ft^b ratio obtained from Eq. (21). Uncertainties we consider to be systematic have not been included. If it is known, then the measured ft^a/ft^b ratio appears in the last column.

Decay pairs, $a; b$	$\delta_R^b - \delta_R^a$ (%)	$\delta_{NS}^b - \delta_{NS}^a$ (%)	$\delta_C^b - \delta_C^a$ (%)	ft^a/ft^b	$(ft^a/ft^b)_{\text{exp}}$
$^{26}\text{Si} \rightarrow ^{26m}\text{Al}; ^{26m}\text{Al} \rightarrow ^{26}\text{Mg}$	0.039	0.215(19)	-0.125(16)	1.00379(25)	1.0048(19)
$^{34}\text{Ar} \rightarrow ^{34}\text{Cl}; ^{34}\text{Cl} \rightarrow ^{34}\text{S}$	0.031	0.089(14)	-0.046(21)	1.00166(25)	1.0028(10)
$^{38}\text{Ca} \rightarrow ^{38m}\text{K}; ^{38m}\text{K} \rightarrow ^{38}\text{Ar}$	0.026	0.069(14)	-0.118(34)	1.00213(36)	1.0037(20)
$^{42}\text{Ti} \rightarrow ^{42}\text{Sc}; ^{42}\text{Sc} \rightarrow ^{42}\text{Ca}$	0.029	0.266(19)	-0.270(57)	1.00565(60)	
$^{46}\text{Cr} \rightarrow ^{46}\text{V}; ^{46}\text{V} \rightarrow ^{46}\text{Ti}$	0.019	0.133(19)	-0.140(82)	1.00292(85)	
$^{50}\text{Fe} \rightarrow ^{50}\text{Mn}; ^{50}\text{Mn} \rightarrow ^{50}\text{Cr}$	0.019	0.111(19)	-0.000(43)	1.00130(47)	
$^{54}\text{Ni} \rightarrow ^{54}\text{Co}; ^{54}\text{Co} \rightarrow ^{54}\text{Fe}$	0.019	0.126(19)	-0.020(85)	1.00165(87)	

where superscript ‘‘a’’ denotes the decay of the $T_z = -1$ parent and ‘‘b’’ denotes the mirror decay of the $T_z = 0$ parent. The expression in Eq. (21) is advantageous because the theoretical uncertainties on the differences, $(\delta_R^b - \delta_R^a)$, $(\delta_{NS}^b - \delta_{NS}^a)$, and $(\delta_C^b - \delta_C^a)$, are all less than on the individual correction terms themselves. For the δ_R^b term this is because its uncertainties are entirely systematic in character. For the structure dependent terms, δ_{NS} and δ_C , it follows from the way that their statistical uncertainties were determined. Several different sets of model parameters were employed to determine each correction term, and the spread in results among the different models was used to establish a ‘‘statistical’’ uncertainty on each. If the same approach is taken to derive an uncertainty on the mirror differences in correction terms, the scatter among the results from the different model parameters is less than the scatter observed in the individual terms.

In Table XV, we present calculated values for the three difference terms that appear in Eq. (21). They are given with their corresponding ft^a/ft^b ratios for the seven pairs of mirror transitions that are included in Table IX. Then, in the last column we show experimental ratios for the three cases that have been measured. The essential information is also illustrated in Fig. 1. It is evident that there is remarkably good agreement between experiment and theory, with a reduced χ^2 of 1.2. The calculated correction terms, or at least those that apply to the six transitions that participate in this mirror test, can be said to have passed another important test.

It would, of course, be valuable to increase the number of measured mirror pairs, but it requires very challenging experiments to characterize the $T_z = -1$ member of each pair to the precision required. The challenge becomes even more acute as these $T_z = -1$ nuclei become farther removed from stability, as they do for the cases with $A \geq 42$. Consequently, one should perhaps not anticipate more mirror pairs being added to those already in Table XV in the near future.

C. Overview

In the preceding sections we have described and tabulated the four correction terms that are required in Eq. (1) to convert an experimental ft value into a corrected $\mathcal{F}t$ value, which can then be used to study the weak-interaction process. To aid in assessing the relative importance of these terms and their uncertainties, we plot them in Fig. 2. Several important

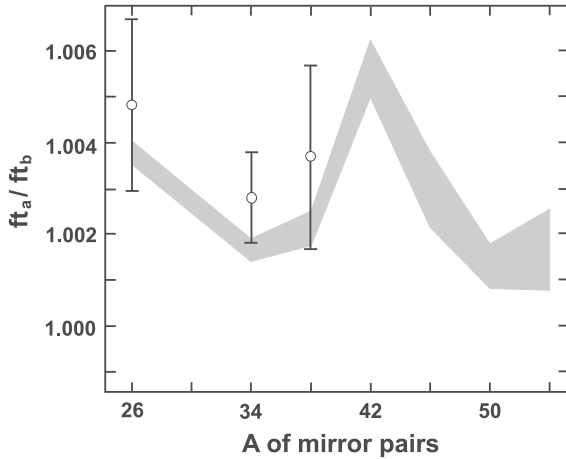


FIG. 1. Calculated and experimental ft^a/ft^b values for the seven mirror pairs of superallowed transitions that appear in Table IX. The gray band connect calculated results taken from Table XV. The measured results for $A = 26, 34,$ and 38 appear as open circles with error bars.

features can be appreciated. First, the two nuclear-structure-dependent terms, δ_C and δ_{NS} , show significant odd-even alternation as well as an overall dependence on Z . Note that δ_{NS} has the opposite sign to δ_C so their odd-even effects reinforce one another since they appear in the form $(\delta_{NS}-\delta_C)$ in Eq. (1).

Second, for all but the lightest nuclei, it is evident that δ'_R is nearly independent of Z even though it is technically a function of both Z and Q_{EC} . Third, for most of the transitions, Δ_R^V and δ'_R are the largest terms and both are essentially unaffected by nuclear properties. Their uncertainties are considered to be systematic in character and thus are not to be applied to individual $\mathcal{F}t$ values but only to their average, $\overline{\mathcal{F}t}$, after it has been obtained.

Finally, since the uncertainties on δ_C are purely statistical, they affect the individual $\mathcal{F}t$ values but their impact

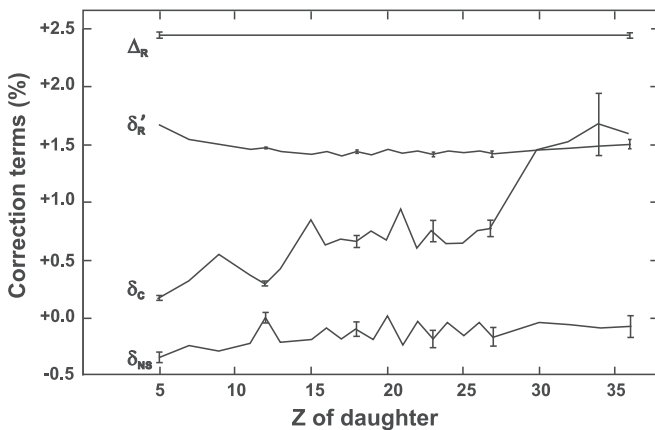


FIG. 2. The calculated correction terms Δ_R^V , δ'_R , δ_C , and δ_{NS} are plotted for each tabulated transition as a function of the atomic number of the daughter nucleus. The lines connecting points serve only to guide the eye. Several representative uncertainties, statistical plus systematic, are shown for each term.

is reduced, when these are averaged. In contrast, the δ_{NS} uncertainties are a mix of both statistical and systematic contributions, with the latter being applied after the averaging. As a result, δ_{NS} turns out to be the predominant contributor to the final uncertainty on $\overline{\mathcal{F}t}$. These points are elaborated in the following sections.

IV. THE $\mathcal{F}t$ VALUES

To obtain the $\mathcal{F}t$ from each ft value, we use Eq. (1) and apply the small transition-dependent correction terms, δ'_R , δ_{NS} , and δ_C . The ft values, correction terms and $\mathcal{F}t$ values all appear in Table XVI. The values we use for δ'_R are listed in column 3, while in column 4 the other two correction terms are combined as $\delta_C-\delta_{NS}$, the way they appear in Eq. (1). The individual values for δ_C and δ_{NS} come from Tables XIV and XI, respectively. In the last column, we present the final derived $\mathcal{F}t$ values. Their uncertainties are statistical only and were derived by our combining the tabulated input uncertainties in quadrature.

A. Consistency of $\mathcal{F}t$ values

Of the 21 $\mathcal{F}t$ values listed in Table XVI, 6 have relative uncertainties greater than $\pm 1.4\%$, too large for the corresponding transitions to play any significant role in current weak-interaction tests. The remaining 15, though, have relative precisions 0.3% or better; and half of them are actually under 0.1%. It is these 15 transitions that we will focus on hereafter.

The uncorrected ft values and fully corrected $\mathcal{F}t$ values for these 15 transitions are plotted as a function of the daughters' atomic numbers in the top and bottom panels, respectively, of Fig. 3. Clearly the correction terms have done a remarkable job of replacing the widely scattered ft values with a set of self-consistent $\mathcal{F}t$ values. This observation is confirmed quantitatively by the weighted average $\overline{\mathcal{F}t}$ of these 15 transitions, which appears at the bottom of the last column of Table XVI: Its χ^2 per degree of freedom is $\chi^2/\nu = 0.47$. Because $\mathcal{F}t$ is inversely proportional to G_V^2 , as is demonstrated by Eq. (1), this result can be said to confirm the constancy of G_V —and to verify this key component of the CVC hypothesis—at the level of 9×10^{-5} . Such excellent consistency among the $\mathcal{F}t$ values is an essential prerequisite for the data to be used in any further probes of the Standard Model.

The uncertainties quoted in Table XVI account only for “statistical” effects, i.e., those that scatter randomly from transition to transition. The δ'_R values appear without uncertainties since, as explained in Sec. III A 2, we consider them to be systematic, i.e., correlated among the 15 transitions. So is one component of the δ_{NS} uncertainties. In Sec. III A 3 we explain why, and separately tabulate the statistical and systematic components for the δ_{NS} uncertainties in Table XI.

We explained and justified our method for dealing with the δ'_R uncertainty in Sec. III A 1 of our 2015 survey [7]. Briefly, we evaluate the individual transition $\mathcal{F}t$'s without including any uncertainties associated with δ'_R , and obtain an average $\overline{\mathcal{F}t}$. Then we shift the individual δ'_R values up and down by one-third of the $Z^2\alpha^3$ contributions, recalculate the $\mathcal{F}t$ values

TABLE XVI. Derived results for superallowed Fermi β decays.

Parent nucleus	$ft(s)$	δ'_R (%)	$\delta_C - \delta_{NS}$ (%)	$\overline{\mathcal{F}t}(s)$
$T_z = -1$				
^{10}C	3042.4 ± 4.1	1.679	0.575 ± 0.039	3075.7 ± 4.4^a
^{14}O	3042.2 ± 0.8	1.543	0.613 ± 0.056	3070.2 ± 1.9^a
^{18}Ne	2912 ± 79	1.506	0.886 ± 0.052	2930 ± 80
^{22}Mg	3051.1 ± 6.9	1.466	0.635 ± 0.026	3076.2 ± 7.0^a
^{26}Si	3052.2 ± 5.6	1.439	0.669 ± 0.033	3075.4 ± 5.7^a
^{30}S	3015 ± 41	1.423	1.001 ± 0.049	3027 ± 41
^{34}Ar	3058.0 ± 2.8	1.412	0.840 ± 0.043	3075.1 ± 3.1^a
^{38}Ca	3062.8 ± 6.0	1.414	0.912 ± 0.049	3077.8 ± 6.2^a
^{42}Ti	3090 ± 88	1.424	1.193 ± 0.066	3097 ± 88
^{46}Cr	3126 ± 100	1.426	0.924 ± 0.089	3141 ± 100
^{50}Fe	3099 ± 71	1.426	0.800 ± 0.053	3118 ± 72
^{54}Ni	3062 ± 50	1.423	0.933 ± 0.070	3077 ± 50
$T_z = 0$				
^{26m}Al	3037.61 ± 0.67	1.478	0.329 ± 0.026	3072.4 ± 1.1^a
^{34}Cl	$3049.43^{+0.95}_{-0.88}$	1.443	0.706 ± 0.051	3071.6 ± 1.8^a
^{38m}K	3051.45 ± 0.92	1.440	0.726 ± 0.056	3072.9 ± 2.0^a
^{42}Sc	3047.7 ± 1.2	1.453	0.657 ± 0.050	3071.7 ± 2.0^a
^{46}V	$3050.33^{+0.54}_{-0.44}$	1.445	0.651 ± 0.063	3074.3 ± 2.0^a
^{50}Mn	3048.4 ± 1.2	1.444	0.689 ± 0.033	3071.1 ± 1.6^a
^{54}Co	$3050.8^{+1.4}_{-1.1}$	1.443	0.787 ± 0.068	$3070.4^{+2.5a}_{-2.4}$
^{62}Ga	3074.1 ± 1.5	1.459	1.49 ± 0.21	3072.4 ± 6.7^a
^{66}As		1.468	1.58 ± 0.40	
^{70}Br		1.486	1.74 ± 0.25	
^{74}Rb	3082.8 ± 6.5	1.499	1.65 ± 0.27	3077 ± 11^a
			Average (best 15), $\overline{\mathcal{F}t}$	3072.24 ± 0.57
			χ^2/ν	0.47

^aValues used to obtain $\overline{\mathcal{F}t}$.

and determine $\overline{\mathcal{F}t}$ for both. The resultant shift in the $\overline{\mathcal{F}t}$ values (± 0.36 s for the data in Table XVI) becomes the systematic uncertainty in $\overline{\mathcal{F}t}$.

We take the same approach in accounting for the systematic component of the δ_{NS} uncertainty, shifting the value of δ_{NS} up and down by its systematic uncertainty and evaluating $\overline{\mathcal{F}t}$ for both. In this case the corresponding systematic uncertainty in $\overline{\mathcal{F}t}$ is ± 1.73 s, much larger than any other contribution to the overall uncertainty.

Thus the final result for $\mathcal{F}t$ becomes

$$\begin{aligned} \overline{\mathcal{F}t} &= 3072.24 \pm 0.57_{\text{stat}} \pm 0.36_{\delta'_R} \pm 1.73_{\delta_{NS}} \text{ s} \\ &= 3072.24 \pm 1.85 \text{ s,} \end{aligned} \quad (22)$$

where the three uncertainties have been combined in quadrature on the second line.

Compared with our 2015 survey result, the new value of $\overline{\mathcal{F}t}$ has hardly changed at all—it is a mere 0.04 s lower—but the uncertainty has increased by a factor of 2.6. This results entirely from the two new terms introduced [188,197] into the calculated δ_{NS} radiative correction (see Sec. III A 3). Although the terms themselves tend to cancel one another, their uncertainties of course add in quadrature, leading to a very large increase in the $\overline{\mathcal{F}t}$ -value uncertainty.

B. Uncertainty budgets

We illustrate the factors which contribute to the individual $\mathcal{F}t$ value uncertainties in two figures. The first, Fig. 4, covers the 15 best-known cases we currently use to determine $\overline{\mathcal{F}t}$; the second, Fig. 5, summarizes the situation for the other 8 cases that are listed in Table XVI. In both figures the first three bars of the five shown for each transition show the contributions from experiment— Q_{EC} values, half lives and branching ratios—while the last two bars refer to the theoretical uncertainties in δ'_R and $\delta_C - \delta_{NS}$. We include contributions from both statistical and systematic uncertainties in the latter two bars, where both play a role.

In Fig. 4, it is immediately evident that, for the transitions from $T_z = 0$ parents, the uncertainties in the structure-dependent correction terms, $\delta_C - \delta_{NS}$, dominate by a substantial margin over the experimental uncertainties. It is a different story for the $T_z = -1$ parent decays, though, where the experimental branching-ratio uncertainties dominate in all cases except that of ^{14}O decay.

The explanation for this difference between the two sets of parents is straightforward. The $T_z = 0$ parents are all odd-odd nuclei, which decay to even-even daughters. Those daughters offer no, or very few, 1^+ states that can be populated by competing Gamow-Teller decays, which means that the branching ratios for their superallowed transitions are $> 99\%$ and can

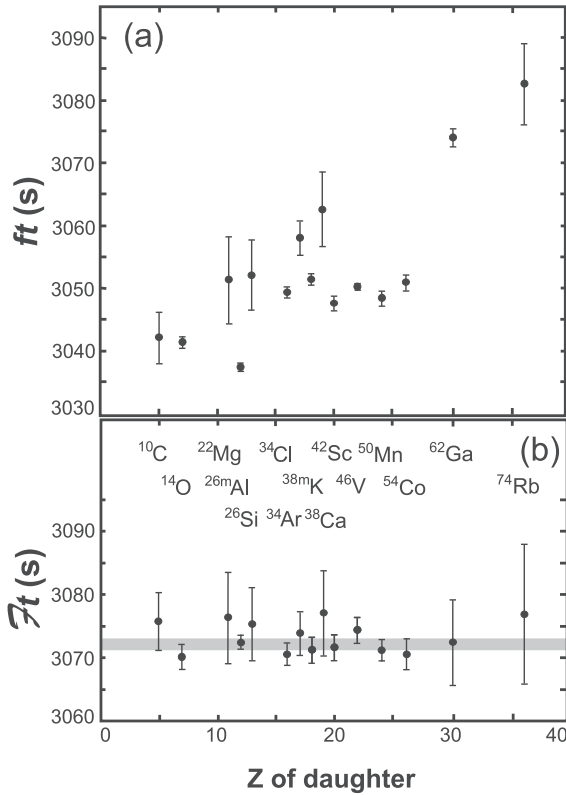


FIG. 3. (a) In the top panel are plotted the uncorrected experimental ft values for the 15 precisely known superallowed transitions as a function of the charge on the daughter nucleus. (b) In the bottom panel, the corresponding Ft values are given; they differ from the ft values by the inclusion of the correction terms δ'_R , δ_{NS} , and δ_C . The horizontal gray band gives one standard deviation around the average Ft value. All transitions are labeled by their parent nuclei.

be established with high precision. Relatively imprecise measurements of the tiny Gamow-Teller branches, which must be subtracted from 100%, are all that is required.

Not so for the decays of the $T_z = -1$ parents. They are even-even nuclei that decay to odd-odd daughters, where 1^+ states are available at low excitation energy. The Gamow-Teller transitions to these states turn out to be strong enough to compete with, and often surpass, the superallowed transitions. This raises a serious experimental challenge: the intensity of the Gamow-Teller branches—or the superallowed branch itself—must be measured directly with high relative precision. Considerable progress has been made in the last few years in improving the measurements of superallowed branching ratios from $T_z = -1$ parents, but they still cannot match the precision of the $T_z = 0$ parents' branching ratios.

The eight cases included in Fig. 5 are much more limited by experiment. All but ^{66}As and ^{70}Br are $T_z = -1$ parents, which will require very difficult measurements to arrive at precise branching ratios. All but ^{18}Ne and ^{30}S are quite far from stability and will be difficult to produce in sufficient quantity for high statistical precision. Overall, the two most advanced candidates are ^{18}Ne and ^{30}S but even they will

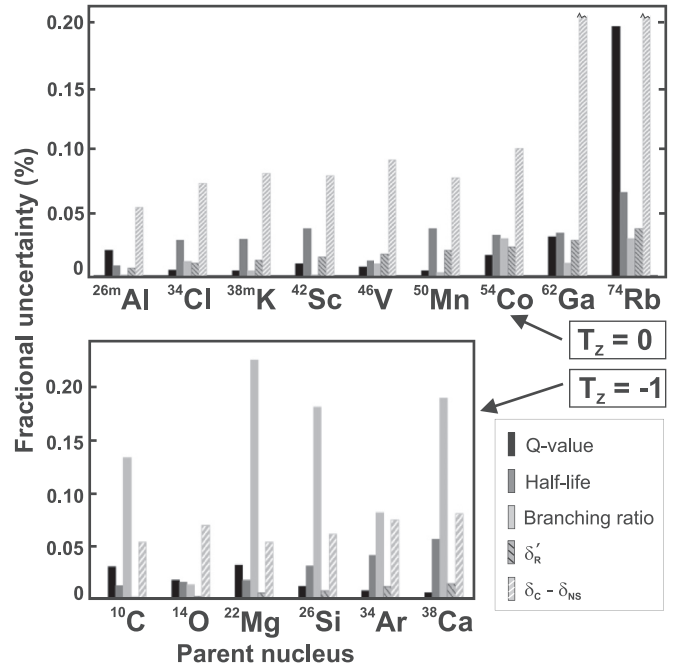


FIG. 4. Summary histogram of the fractional uncertainties attributable to each experimental and theoretical input factor that contributes to the final Ft values for the 15 precisely measured superallowed transitions used in the Ft -value average. The two bars cut off with jagged lines at about 0.20% actually rise to 0.23% for ^{62}Ga and 0.29% for ^{74}Rb . The bars for δ'_R and $\delta_C - \delta_{NS}$ include provision for systematic uncertainty as well as statistical. See text.

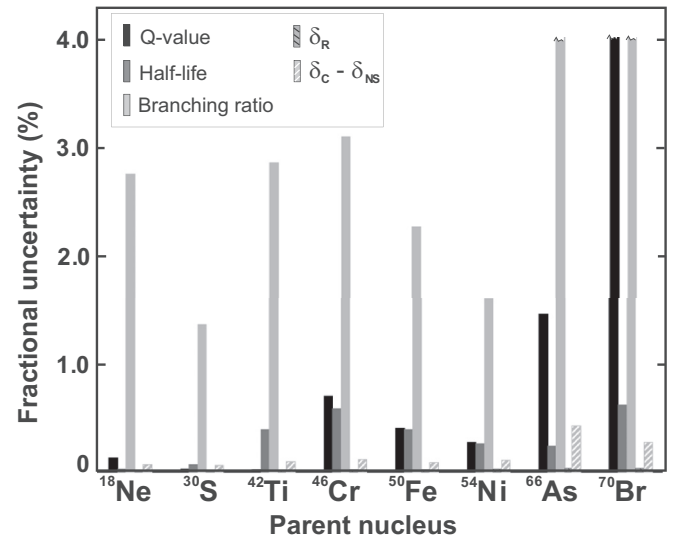


FIG. 5. Summary histogram of the fractional uncertainties attributable to each experimental and theoretical input factor that contributes to the final Ft values for the eight tabulated superallowed transitions not known precisely enough to contribute to the Ft -value average. The three bars cut off with jagged lines at about 4.0% indicate that no useful experimental measurement has been made of those parameters. The bars for δ'_R and $\delta_C - \delta_{NS}$ include provision for systematic uncertainty as well as statistical. See text.

require considerable experimental effort before they can become competitive with the 15 decays that are already well known.

Most importantly, there is no reason to believe that experimenters have reached the limit of achievable precision even for the best cases shown in Fig. 4, but until some improvement can be made by theorists in the calculated structure-dependent correction terms, δ_C - δ_{NS} , there is little motivation to take more extraordinary measures.

V. IMPACT ON WEAK-INTERACTION PHYSICS

A. Value of V_{ud}

In Sec. IV we determined precise $\overline{\mathcal{F}t}$ values for 15 superallowed transitions, and established their conformity with the CVC expectation that they should all agree within statistics. This agreement justified our taking an average of all 15 results to obtain $\overline{\mathcal{F}t}$, from which the vector coupling constant G_V can be calculated via Eq. (1). Though uninteresting in itself, G_V in combination with the weak-interaction constant for the purely leptonic muon decay, G_F , yields a value for V_{ud} , which is the much more interesting up-down element of the CKM quark-mixing matrix. The basic relationship, $V_{ud} = G_V/G_F$, can be cast in terms of $\overline{\mathcal{F}t}$ with the help of Eq. (1) as follows:

$$\begin{aligned} |V_{ud}|^2 &= \frac{K}{2G_F^2(1 + \Delta_R^V)\overline{\mathcal{F}t}} \\ &= \frac{2912.95 \pm 0.54}{\overline{\mathcal{F}t}}, \end{aligned} \quad (23)$$

where we have used the MuLan value for the weak interaction coupling constant from muon decay [182,203], $G_F/(\hbar c)^3 = 1.1663787(6) \times 10^{-5} \text{ GeV}^{-2}$; and the value for Δ_R^V , the nucleus-independent radiative correction, is taken from Eq. (10). Substituting the result for $\overline{\mathcal{F}t}$ from Eq. (22) we obtain

$$|V_{ud}|^2 = 0.94815 \pm 0.00060. \quad (24)$$

The uncertainty attached to $|V_{ud}|^2$ in Eq. (24) includes contributions from many sources but is completely dominated by those originating from the theoretical correction terms, with experiment contributing a mere 0.00009 to the 0.00060 total. Among the theoretical uncertainties, δ_{NS} contributes the most, at 0.00053; Δ_R^V is next with 0.00018; δ_R' is responsible for 0.00011 and δ_C contributes least, with 0.00008.

The situation has changed significantly since our last review in 2015 [7]. Two new calculations of Δ_R^V [187–189] have appeared in the interim. As described in Sec. III A 1, the uncertainty on that correction has consequently been reduced—and its value has been changed significantly in the process. This has had the effect of reducing the magnitude of V_{ud} . At the same time, we see from Sec. III A 3 that two new contributions to δ_{NS} [188,197] have also been introduced. Since they tend to cancel one another, they have had very little effect on the magnitude of V_{ud} , but their uncertainties are large and, when combined, they are enough to substantially increase the V_{ud} uncertainty and make δ_{NS} by far its largest contributor.

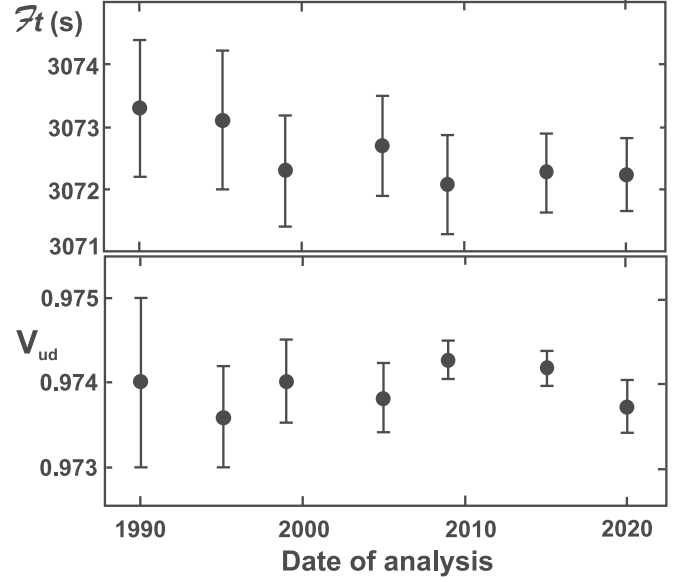


FIG. 6. Values of $\overline{\mathcal{F}t}$ and V_{ud} as determined from superallowed $0^+ \rightarrow 0^+$ β decays plotted as a function of analysis date, spanning the past three decades. Only the statistical uncertainties are shown for the $\overline{\mathcal{F}t}$ values. In order, from the earliest date to the most recent, the values are taken from Refs. [4,204,205,5–7] and this work.

The value of V_{ud} corresponding to the result in Eq. (24) is

$$|V_{ud}| = 0.97373 \pm 0.00031. \quad (25)$$

How this compares with the values we have obtained for $|V_{ud}|$ from superallowed β decay in the past is illustrated in the bottom panel of Fig. 6, which covers a span of three decades. The top panel of the figure traces the corresponding $\overline{\mathcal{F}t}$ -value history over the same time period. From the $\overline{\mathcal{F}t}$ behavior, we can conclude that the experimental results have been very stable, with steady improvements in precision as new transitions were added and old ones refined. World data on superallowed β decay has proven to be a truly robust set. Overall, the behavior of $|V_{ud}|$ is quite reasonable, too. Successive values have all been within the uncertainties of previous values and, until now, the uncertainties themselves have been steadily decreasing. The increased uncertainty and larger-than-usual change in its value evident in the present result, are due to changes in the theoretical correction terms, which we have already described.

B. Value of V_{us}

The most precise values of V_{us} are derived from the leptonic and semileptonic decays of the kaon. Other determinations based on hyperon decays and hadronic τ decays will not be considered here.

For the semileptonic $K \rightarrow \pi \ell \nu_\ell$ decays, denoted $K_{\ell 3}$, there are five measured decay channels, which involve charged or neutral kaons decaying either to electrons or muons. Results from the different decay channels have been evaluated by the FlaviaNet group [206] with more recent updates provided by Moulson [207]. The currently accepted average from all five

TABLE XVII. Lattice QCD values for $f_+(0)$ and f_K/f_π appear in columns 2 and 3, respectively, distinguished by the number of quark flavors present in the simulations. The values are taken from FLAG19 [211] with updates provided by Moulson [207]. The deduced values of $|V_{us}|$ (from $K_{\ell 3}$ decays) and $|V_{us}|/|V_{ud}|$ (from $K_{\ell 2}$ decays) appear in columns 4 and 5, respectively. The corresponding unitarity sums are in column 6, with the residuals, Δ_{CKM} in column 7. The number of standard deviations, σ , of the discrepancy with unitarity, if any, appears in column 8. Rows 5 and 6 give $|V_{us}|$ obtained by our fitting three data: $|V_{ud}|$ from β decay, $|V_{us}|$ from $K_{\ell 3}$ decays, and $|V_{us}|/|V_{ud}|$ from $K_{\ell 2}$ decays, with two free parameters, $|V_{ud}|$ and $|V_{us}|$, for each of the specified value of N_f . The Particle Data Group $|V_{us}|$ value [210] is given in the last line.

	$f_+(0)$	f_K/f_π	$ V_{us} $	$ V_{us} / V_{ud} $	$ V_u ^2$	Δ_{CKM}	σ
$N_f = 2 + 1 + 1$	0.9698(17)		0.22326(58)		0.99801(65)	-0.00199(65)	3.1
$N_f = 2 + 1$	0.9677(27)		0.22375(75)		0.99823(69)	-0.00177(69)	2.6
$N_f = 2 + 1 + 1$		1.1967(18)		0.23129(45)	0.99889(66)	-0.00111(66)	1.7
$N_f = 2 + 1$		1.1946(34)		0.23170(72)	0.99907(70)	-0.00093(70)	1.3
$N_f = 2 + 1 + 1$			0.22449(95)		0.99841(165)	-0.00159(165)	
$N_f = 2 + 1$			0.22475(93)		0.99860(116)	-0.00140(116)	1.2
PDG 18			0.2243(5)		0.9985(6)	-0.0015(6)	2.4

channels is

$$|V_{us}|f_+(0) = 0.21652(41), \quad (26)$$

where $f_+(0)$ is the semileptonic decay form factor at zero-momentum transfer.

For purely leptonic kaon decays, $K^\pm \rightarrow \mu^\pm \nu$, denoted $K_{\ell 2}$, the critical feature is that the measurements are expressed as ratios to leptonic pion decays $\pi^\pm \rightarrow \mu^\pm \nu$ because many hadronic uncertainties are minimized in the ratio. With certain long-distance electromagnetic corrections, δ_{EM} , put aside for the moment, the ratio of decay rates leads to a value of $(|V_{us}|/|V_{ud}|) \times (f_{K^\pm}/f_{\pi^\pm})$, where the ratio of decay constants f_{K^\pm}/f_{π^\pm} includes the effects of strong isospin breaking: $f_{K^\pm}/f_{\pi^\pm} = (f_K/f_\pi) \times [1 + \delta_{\text{SU}(2)}]^{1/2}$. Recent lattice simulations [208,209] are able to provide a result for the combined correction, $\delta_{\text{EM}} + \delta_{\text{SU}(2)}$. With this correction included, Moulson [207] recommends the experimental $K_{\ell 2}$ result be taken as

$$\frac{|V_{us}|}{|V_{ud}|} \frac{f_K}{f_\pi} = 0.27679(34). \quad (27)$$

To extract V_{us} from the results in either Eq. (26) or Eq. (27), lattice QCD calculations are required in order to evaluate the form factor $f_+(0)$ in the former, and the ratio of decay constants f_K/f_π in the latter. The Flavor Lattice Averaging Group (FLAG) provides timely updates on the status of lattice calculations. In Table XVII we present, in columns 2 and 3, the results from their most recent report, FLAG19 [211], once again with even more recent updates from Moulson [207]. Results appear as a function of N_f , the number of quark flavors included in the lattice simulations, where we consider results both for three quark flavors, $N_f = 2 + 1$, and for four, $N_f = 2 + 1 + 1$. We do not attempt to average one with the other since the FLAG collaboration recommends against it.

In the first four rows of columns 4 and 5 of the table we give the values of $|V_{us}|$ and $|V_{us}|/|V_{ud}|$ that correspond to the lattice calculations in the preceding two columns. It is important to recognize that the two sets of results, from $K_{\ell 3}$ and $K_{\ell 2}$ decays, are statistically inconsistent with one another. For example, if the $N_f = 2 + 1 + 1$ result for $|V_{us}|/|V_{ud}|$, 0.23129, is multiplied by the value of $|V_{ud}|$ from Eq. (25), then the result

for $|V_{us}|$ becomes 0.22522(44), which differs by three standard deviations from the $N_f = 2 + 1 + 1$ result for $|V_{us}|$.

Nevertheless, we combine these two sets of data to yield a best-fit $|V_{us}|$ by proceeding as follows: With the values of $|V_{us}|$ from $K_{\ell 3}$ decays, $|V_{us}|/|V_{ud}|$ from $K_{\ell 2}$ decays, and $|V_{ud}|$ from nuclear β decay, we have three pieces of data from which to determine two parameters, $|V_{ud}|$ and $|V_{us}|$. To do so, we performed nonlinear least-squares fits to obtain values of $|V_{us}|$ given in rows 5 and 6 of column 4 in the table. For the reason described in the preceding paragraph, the χ^2 of each fit was poor, being 3.28 and 7.24 for the $N_f = 2 + 1$ and $N_f = 2 + 1 + 1$ cases, respectively. The uncertainties assigned to $|V_{us}|$ have been scaled appropriately by the square root of the χ^2 . The corresponding fit values for $|V_{ud}|$ undergo very small shifts from the precisely specified β decay value, but their uncertainties are significantly scaled: $|V_{ud}| = 0.97369(55)$ for the $N_f = 2 + 1$ calculations and $|V_{ud}| = 0.97365(82)$ for the $N_f = 2 + 1 + 1$ version.

In the last line of Table XVII we give the 2018 recommended value of the Particle Data Group [210], which is based on the $N_f = 2 + 1 + 1$ lattice simulations available at the time for the form factor $f_+(0)$ and decay constants f_K/f_π . Their recommended average $|V_{us}| = 0.2243(5)$ is a weighted average of 0.2231(8) from $K_{\ell 3}$ and 0.2253(7) from $K_{\ell 2}$ data. The difference between our results and theirs simply reflects the impact of new lattice calculations that have appeared in the past year.

C. CKM unitarity

It is an important tenet of the standard model that the CKM matrix should be unitary. Thus, it is of paramount importance to test whether this tenet stands up to experimental scrutiny. To date, the most demanding way to test CKM unitarity is to sum the squares of the measured values of its top-row elements,

$$|V_u|^2 = |V_{ud}|^2 + |V_{us}|^2 + |V_{ub}|^2 = 1 + \Delta_{\text{CKM}}, \quad (28)$$

which should equal exactly 1, with the residual Δ_{CKM} being zero if the matrix is unitary. Because $|V_{ud}|^2$ accounts for 95% of this sum, its precision is of the greatest importance.

In our 2015 survey [7], the unitarity condition was well satisfied, but since then the value of $|V_{ud}|$ has been lowered and its precision worsened by changes in, and additions to, the calculated radiative corrections. This leads to an appreciable reduction in the unitarity sum.

Values of $|V_{us}|$ discussed in Sec. VB have improved in precision since our last survey mainly because of improved precision in the lattice simulations for the form factor and decay constants. But that has had the unfortunate effect of enhancing the disagreement between the results from the $K_{\ell 3}$ and $K_{\ell 2}$ decays. In the end, the net outcome is to increase the unitarity-sum uncertainty.

The third element of the top row, $|V_{ub}|$, is very small and hardly impacts the unitarity test at all. Its value from the Particle Data Group (PDG) evaluation [182] is

$$|V_{ub}| = (3.94 \pm 0.36) \times 10^{-3}. \quad (29)$$

Our approach to the unitarity test in the past has been to combine our result for $|V_{ud}|$ with the PDG evaluated results for $|V_{us}|$ and $|V_{ub}|$. This result is given in the last line of Table XVII, where the unitarity sum is $|V_u|^2 = 0.9985(6)$ showing a failure to meet unitarity by 2.4σ . However, since the PDG 2018 report was written there has been considerable activity especially in lattice simulations. The most recent results available to us are in the top four rows of Table XVII so we focus our attention on those.

In rows 1 and 2, we use $|V_{us}|$ from $K_{\ell 3}$ decays, together with our $|V_{ud}|$ value from Eq. (25), to obtain unitarity sums of 0.99823(69) and 0.99801(65) for, respectively, $N_f = 2 + 1$ and $N_f = 2 + 1 + 1$ lattice calculations of $f_+(0)$. These results indicate a failure of unitarity of around 2.8σ . This failure of the $K_{\ell 3}$ result to agree with unitarity has been apparent for some time and was already noted in our 2015 survey [7]. However, the discrepancy with unitarity has now been compounded by the smaller value of $|V_{ud}|$ reported here.

In rows 3 and 4, we use $|V_{us}|/|V_{ud}|$ from $K_{\ell 2}$ decays and our $|V_{ud}|$ result from Eq. (25) to obtain unitarity sums of 0.99907(70) and 0.99889(66) for, respectively, $N_f = 2 + 1$ and $N_f = 2 + 1 + 1$ lattice calculations for the decay constants, f_K/f_π . Again, we see a unitarity breakdown, albeit a smaller one, of around 1.5σ . In the past, $K_{\ell 2}$ data have yielded $|V_{us}|/|V_{ud}|$ values consistent with unitarity, but the smaller value of $|V_{ud}|$ reported here has opened up a discrepancy here, too.

Last, in lines 5 and 6 we try to reconcile the results from $K_{\ell 2}$ and $K_{\ell 3}$ decays by combining all three pieces of data— $|V_{us}|$ from $K_{\ell 3}$ decays, $|V_{us}|/|V_{ud}|$ from $K_{\ell 2}$ decays, and $|V_{ud}|$ from β decays—to extract a best fit to the two parameters $|V_{us}|$ and $|V_{ud}|$. Because the input data are statistically inconsistent with one another, the revised $|V_{us}|$ and $|V_{ud}|$ outputs have acquired much larger uncertainties. The unitarity sums obtained are 0.99860(116) and 0.99841(165) for $N_f = 2 + 1$ and $N_f = 2 + 1 + 1$ lattice calculations, respectively. Although these unitarity sums are similar in magnitude to the others in the table, their larger uncertainties superficially restore agreement with unitarity.

In conclusion, there are strong hints that the currently accepted data for V_{ud} and V_{us} fall short of unitarity by 2σ or

possibly more, but the incompatibility of the $K_{\ell 3}$ and $K_{\ell 2}$ results for $|V_{us}|$ make a definitive conclusion elusive. Certainly, the $|V_{ud}|$ value reported here has had the effect of increasing tension in the unitarity test. Overall, the new data have opened up some space for those seeking hints of physics beyond the standard model.

D. Scalar currents

1. Fundamental scalar currents

The standard model prescribes the weak interaction to be an equal mix of vector (V) and axial-vector (A) interactions that maximize parity violation. Searches for physics beyond the standard model therefore seek evidence that parity is not maximally violated or that the interaction is not pure $V-A$; admitting, for example, the presence of scalar (S) and/or tensor (T) contributions. By being restricted to $0^+ \rightarrow 0^+$ β transitions, the data in this survey only access the vector sector and are sensitive to a possible contribution from scalar interactions.

A general form of the weak-interaction Hamiltonian, written by Jackson, Treiman, and Wyld [212] for vector and scalar interactions, is

$$H_{S+V} = (\bar{\psi}_p \psi_n)(C_S \bar{\phi}_e \phi_{\bar{\nu}_e} + C'_S \bar{\phi}_e \gamma_5 \phi_{\bar{\nu}_e}) + (\bar{\psi}_p \gamma_\mu \psi_n)[C_V \bar{\phi}_e \gamma_\mu (1 + \gamma_5) \phi_{\bar{\nu}_e}], \quad (30)$$

where we have retained the notation and metric of Ref. [212]. As determined by experiment, the vector current in this equation is taken to be maximally parity violating. In the following discussion, we will also take the most restrictive conditions for the scalar currents: We will assume that, like the vector current, it is time-reversal invariant (i.e., C_S and C_V are real) and it is maximally parity violating (i.e., $C_S = C'_S$).² In this way, we are left with one new parameter, C_S , whose value we can constrain from our data on superallowed β decays.

As discussed in detail in Ref. [5], a scalar interaction would add an additional term to the shape-correction function, which is part of the integrand of the statistical rate function, f . The function f is an integral over β -decay phase space and this additional term depends inversely on W , the total electron energy in electron rest-mass units. Thus, the impact of a scalar interaction on f values—and therefore on $\mathcal{F}t$ —would be to introduce a dependence on $\langle 1/W \rangle$, the average inverse decay energy of each transition. No longer would the $\mathcal{F}t$ values be constant over the whole range of nuclei, but they would instead exhibit a smooth dependence on $\langle 1/W \rangle$. Since $\langle 1/W \rangle$ is largest for light nuclei and decreases smoothly with increasing Z and A , the largest deviation of $\mathcal{F}t$ from constancy in our data would occur for the cases of ^{10}C and ^{14}O .

We have reevaluated the statistical rate function f for each transition using a shape-correction function that includes the presence of a scalar interaction. We then obtain a value of C_S that minimizes the χ^2 in a fit to the expression $\mathcal{F}t = \text{const.}$

²Of course, $C_S = -C'_S$ would also be maximally parity violating but in that case superallowed β decay would be completely insensitive to any contribution from a scalar current.

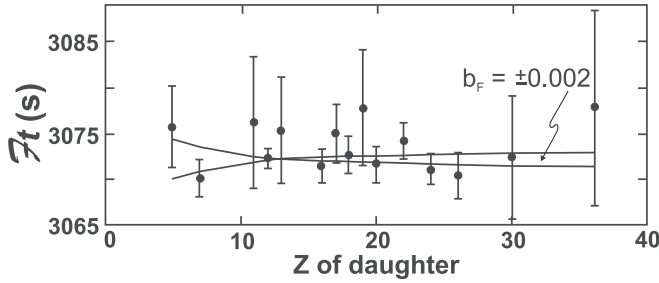


FIG. 7. Corrected $\mathcal{F}t$ values from Table XVI plotted as a function of the charge on the daughter nucleus, Z . The curved lines represent the approximate loci the $\mathcal{F}t$ values would follow if a scalar current existed with $b_F = \pm 0.002$.

The result we obtained is

$$b_F = -2 \frac{C_S}{C_V} = 0.0000 \pm 0.0020, \quad (31)$$

where b_F is the historic Fierz interference term [212], which is simply twice C_S/C_V under the restrictive assumptions that the scalar interaction is both time-reversal invariant and maximally parity violating. The uncertainty quoted in Eq. (31) is one standard deviation (68% CL). At the 90% confidence level, this result corresponds to

$$|b_F| \leq 0.0033, \quad (32)$$

a limit which is a factor-of-two tighter than the one we obtained in our last survey [7].

There were two free parameters in this fit to the data: C_S/C_V and $\overline{\mathcal{F}t}$. Corresponding to the result for the former, which is quoted in Eq. (31), is $\overline{\mathcal{F}t} = 3072.3 \pm 1.6$ s, the result for the latter. Note that only statistical uncertainties are relevant here. This result compares well to $\overline{\mathcal{F}t} = 3072.24 \pm 0.57$ s (see Table XVI) the value we obtained without introducing a scalar current. The central value is essentially unchanged but the uncertainty in a two-parameter fit increases by a factor of nearly three.

In Fig. 7 we illustrate the sensitivity of this analysis by plotting the measured $\mathcal{F}t$ values together with the loci of $\mathcal{F}t$ values that would be expected if $b_F = \pm 0.002$, the present uncertainty limits.

2. Induced scalar currents

If we only consider the vector part of the weak interaction, then for composite spin-1/2 nucleons, as opposed to pointlike quarks, its most general form is written [213]

$$H_V = \overline{\psi}_p (g_V \gamma_\mu - f_M \sigma_{\mu\nu} q_\nu + i f_S q_\mu) \psi_n \overline{\phi}_e \gamma_\mu (1 + \gamma_5) \phi_{\overline{\nu}_e}, \quad (33)$$

with q_μ being the four-momentum transfer between hadrons and leptons. The values of the coupling constants g_V (vector), f_M (weak magnetism), and f_S (induced scalar) are pre-determined if the CVC hypothesis is correct in prescribing that the weak vector current is just an isospin rotation of the electromagnetic vector current. In particular, because CVC implies that the vector current is divergenceless, the induced scalar term f_S should be identically zero.

The Hamiltonian in Eq. (33) can be reorganized to match exactly the form given by Jackson, Treiman, and Wyld, Eq. (30), with C_S replaced by $m_e f_S$ and C_V with g_V . Here m_e is the electron rest mass, which is $m_e = 1$ in the electron rest-mass units we use. Thus, the value of C_S/C_V in Eq. (31) equally applies to $m_e f_S/g_V$,

$$\left| \frac{m_e f_S}{g_V} \right| \leq 0.0016, \quad (34)$$

at the 90% confidence level. This result is a vindication of the CVC hypothesis, which predicts that $g_V = 1$ and $f_S = 0$.

VI. CONCLUSIONS

Since our last survey in 2015, a large number of new measurements have been reported. In some cases, these have served to improve the precision with which a few key transitions are known; in others, they have demonstrated that new transitions are becoming accessible to good-quality experiments. In the first category are new measurements of the ^{14}O branching ratio [166] and Q_{EC} value [168], as well as the ^{10}C half-life [56], all of which reduce uncertainties on the $\mathcal{F}t$ values for the low- Z parents that are key to establishing a tight limit on the Fierz term b_F (see Sec. VD 1). In the same category are the precise branching-ratio results for ^{26}Si [36] and ^{34}Ar [107], which have now tripled the number of mirror superallowed transitions that are well characterized. The ft -value ratios for these mirror pairs have provided a stringent new test of the efficacy of the nuclear-structure-dependent correction terms (see Sec. III B 2).

In the second category of significant recent measurements are two that have led to three new $T_Z = -1$ superallowed emitters, ^{46}Cr , ^{50}Fe , and ^{54}Ni , being added to our tables for the first time. Although the results obtained so far [129,179] are not precise enough for these superallowed transitions to be used in the extraction of V_{ud} (see Table XVI), they do demonstrate that these parent nuclei are potential candidates for future more-precise measurements.

Of equal or greater import are recent reevaluations of the radiative correction terms, δ_{NS} and Δ_R^V . Two new contributors to δ_{NS} have been identified and their magnitudes calculated approximately [188,197]. The two contributions effectively cancel one another, but unfortunately both carry relatively large uncertainties, which cause the overall uncertainty on δ_{NS} to increase significantly, even though its magnitude remains largely unchanged (see Sec. III A 3). In contrast, two new calculations of Δ_R^V by Seng *et al.* [187,188] and by Czarnecki *et al.* [189] have led to an important reduction in its uncertainty but have increased its magnitude by more than twice the uncertainty assigned to its previous value (see Table X).

The impact these changes have made on the final values we now obtain for the average $\overline{\mathcal{F}t}$ and for V_{ud} are illustrated in Fig. 6. On the one hand, the value of $\overline{\mathcal{F}t}$ with statistical uncertainties has hardly changed at all from our 2015 survey, indicating that the body of world experimental data is very robust; but, on the other hand, the value of V_{ud} has decreased appreciably because of the increase in Δ_R^V , and its uncertainty has increased as a result of the enlarged δ_{NS} uncertainty.

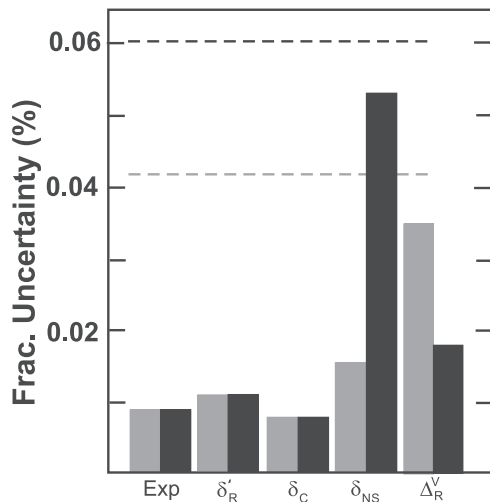


FIG. 8. Uncertainty budget for $|V_{ud}|^2$ as obtained from superallowed $0^+ \rightarrow 0^+$ β decay. The contributions are separated into five categories: experiment, the transition-dependent part of the radiative correction (δ_R^V), the nuclear-structure-dependent terms δ_C and δ_{NS} , and the transition-independent part of the radiative correction Δ_R^V . The gray bars give the contributions in 2015 [7] while the black bars represent the present survey. The gray and black dashed lines give the corresponding total uncertainties.

It is instructive to examine Fig. 8, which shows the complete uncertainty budget for $|V_{ud}|^2$ and compares it with the same accounting taken in 2015 [7]. The most striking observation is that theory remains by far the largest contributor to the $|V_{ud}|^2$ uncertainty but that the chief culprit has changed from being Δ_R^V to being δ_{NS} . For years we have called for improvements to the calculation of Δ_R^V , and it is gratifying that two new calculations have resulted in its uncertainty being reduced to the point where it is now only a factor of two greater than the uncertainty on the collected experimental results. Unfortunately though, the uncertainty on δ_{NS} has grown more than Δ_R^V 's has shrunk. This is because the two new small effects that have been added to δ_{NS} were only quantified with relatively crude nuclear models, which necessarily brought with them rather large uncertainties. We urge that these models be refined in future so that the uncertainty on δ_{NS} can be brought more in line with the other four contributors to the $|V_{ud}|^2$ uncertainty.

In fact, it has to be admitted that the motivation for a new generation of experiments to improve the ft values still further will be very weak until the theoretical uncertainties associated with δ_{NS} have been reduced substantially. Currently the δ_{NS} uncertainty exceeds the overall experimental one by nearly a factor of six. It is clear where future priorities must lie!

While the value for V_{ud} has become somewhat less precise than it appeared to be five years ago, over the same time span we have seen a real improvement in the limit on the Fierz interference term. Whereas the 90% confidence limit 5 years ago was $|b_F| \leq 0.0070$, it has now been reduced by a factor of two, to $|b_F| \leq 0.0033$. This limit on the ratio of scalar-to-vector currents is by a wide margin the tightest available anywhere. It remains the best evidence we have that the standard model is correct in ruling out the presence of a scalar current. The significantly reduced limit has come from new measurements on the superallowed transitions from ^{10}C and ^{14}O . Further progress is still possible if some courageous team can mount a successful experiment to improve the measured branching-ratio for the ^{10}C superallowed branch.

Note added in proof. A new measurement of the superallowed branching ratio of ^{10}C was published several months after the closing date of our survey and this manuscript's submission to the journal (see Ref. [214]). The new result, 1.4638(50)%, agrees well with the world average in Table IV and is substantially less precise than the two most precise previous measurements of the same quantity. It has no impact on our survey results.

ACKNOWLEDGMENTS

As the authors are both now retired, this critical survey of superallowed $0^+ \rightarrow 0^+$ β decays will be our last. In the 50 years we have worked in and surveyed this exciting field, we have benefited immeasurably from working with collaborators and colleagues. They are too numerous to name individually, but we extend to all of them our profound appreciation.

This material is based on work supported by the U.S. Department of Energy, Office of Science, Office of Nuclear Physics, under Award No. DE-FG03-93ER40773, and by the Robert A. Welch Foundation under Grant No. A-1397.

[1] I. S. Towner and J. C. Hardy, *Nucl. Phys. A* **205**, 33 (1973).
 [2] J. C. Hardy and I. S. Towner, *Nucl. Phys. A* **254**, 221 (1975).
 [3] V. T. Koslowsky, E. Hagberg, J. C. Hardy, H. Schmeing, R. E. Azuma, and I. S. Towner, in *Proceedings of the 7th International Conference on Atomic Masses and Fundamental Constants*, edited by O. Klepper (Technische Hochschule Darmstadt, 1984), p. 572.
 [4] J. C. Hardy, I. S. Towner, V. T. Koslowsky, E. Hagberg, and H. Schmeing, *Nucl. Phys. A* **509**, 429 (1990).
 [5] J. C. Hardy and I. S. Towner, *Phys. Rev. C* **71**, 055501 (2005); *Phys. Rev. Lett.* **94**, 092502 (2005).

[6] J. C. Hardy and I. S. Towner, *Phys. Rev. C* **79**, 055502 (2009).
 [7] J. C. Hardy and I. S. Towner, *Phys. Rev. C* **91**, 025501 (2015).
 [8] E. G. Adelberger, M. M. Hindi, C. D. Hoyle, H. E. Swanson, R. D. Von Lintig, and W. C. Haxton, *Phys. Rev. C* **27**, 2833 (1983); this reference replaces the result reported in E. G. Adelberger, C. D. Hoyle, H. E. Swanson, and R. D. Von Lintig, *Phys. Rev. Lett.* **46**, 695 (1981).
 [9] F. Ajzenberg-Selove, *Nucl. Phys. A* **490**, 1 (1988).
 [10] F. Ajzenberg-Selove, *Nucl. Phys. A* **523**, 1 (1991).
 [11] D. E. Alburger, *Phys. Rev. C* **5**, 274 (1972).

- [12] D. E. Alburger and F. P. Calaprice, *Phys. Rev. C* **12**, 1690 (1975).
- [13] D. E. Alburger and D. H. Wilkinson, *Phys. Rev. C* **15**, 2174 (1977); this reference replaces the ^{46}V half-life from [175].
- [14] D. E. Alburger, *Phys. Rev. C* **18**, 1875 (1978).
- [15] P. F. A. Alkemade, C. Alderliesten, P. De Wit, and C. Van der Leun, *Nucl. Instrum. Methods* **197**, 383 (1982).
- [16] G. Azuelos, J. E. Crawford, and J. E. Kitching, *Phys. Rev. C* **9**, 1213 (1974).
- [17] G. Azuelos and J. E. Kitching, *Phys. Rev. C* **12**, 563 (1975).
- [18] R. K. Barden, C. A. Barnes, W. A. Fowler, and P. G. Seeger, *Phys. Rev.* **127**, 583 (1962).
- [19] P. H. Barker, C. J. Scofield, R. J. Petty, J. M. Freeman, S. D. Hoath, W. E. Burcham, and G. T. A. Squier, *Nucl. Phys. A* **275**, 37 (1977); the same result also appears in G. T. A. Squier, W. E. Burcham, S. D. Hoath, J. M. Freeman, P. H. Barker, and R. J. Petty, *Phys. Lett. B* **65**, 122 (1976).
- [20] P. H. Barker and J. A. Nolen, in *Proceedings of the International Conference on Nuclear Structure, Tokyo, Sept. 5–10, 1977* (International Academic Publishing Co. Ltd., Tokyo, 1977).
- [21] P. H. Barker and R. E. White, *Phys. Rev. C* **29**, 1530 (1984).
- [22] P. H. Barker and S. M. Ferguson, *Phys. Rev. C* **38**, 1936 (1988).
- [23] S. C. Baker, M. J. Brown, and P. H. Barker, *Phys. Rev. C* **40**, 940 (1989).
- [24] P. H. Barker and G. D. Leonard, *Phys. Rev. C* **41**, 246 (1990).
- [25] P. H. Barker and P. A. Amundsen, *Phys. Rev. C* **58**, 2571 (1998); this reference updates the $^{10}\text{C} Q_{\text{EC}}$ -value from Ref. [23]; its value for the $^{14}\text{O} Q_{\text{EC}}$ value was later withdrawn in Ref. [163].
- [26] P. H. Barker and M. S. Wu, *Phys. Rev. C* **62**, 054302 (2000).
- [27] G. C. Ball, S. Bishop, J. A. Behr, G. C. Boisvert, P. Bricault, J. Cerny, J. M. D'Auria, M. Dombisky, J. C. Hardy, V. Iacob, J. R. Leslie, T. Lindner, J. A. Macdonald, H.-B. Mak, D. M. Moltz, J. Powell, G. Savard, and I. S. Towner, *Phys. Rev. Lett.* **86**, 1454 (2001).
- [28] P. H. Barker, I. C. Barnett, G. J. Baxter, and A. P. Byrne, *Phys. Rev. C* **70**, 024302 (2004).
- [29] P. H. Barker and A. P. Byrne, *Phys. Rev. C* **73**, 064306 (2006).
- [30] P. H. Barker, K. K. H. Leung, and A. P. Byrne, *Phys. Rev. C* **79**, 024311 (2009).
- [31] G. C. Ball, G. Boisvert, P. Bricault, R. Churchman, M. Dombisky, T. Lindner, J. A. Macdonald, E. Vandervoort, S. Bishop, J. M. D'Auria, J. C. Hardy, V. E. Iacob, J. R. Leslie, and H.-B. Mak, *Phys. Rev. C* **82**, 045501 (2010).
- [32] I. Berka, K. P. Jackson, C. Rolfs, A. M. Charlesworth, and R. E. Azuma, *Nucl. Phys. A* **288**, 317 (1977).
- [33] J. A. Becker, R. A. Chalmers, B. A. Watson, and D. H. Wilkinson, *Nucl. Instrum. Methods* **155**, 211 (1978).
- [34] F. J. Bergmeister, K. P. Lieb, K. Pampus, and M. Uhrmacher, *Z. Phys. A* **320**, 693 (1985).
- [35] A. Bey, B. Blank, G. Canchel, C. Dossat, J. Giovinazzo, I. Matea, V.-V. Elomaa, T. Eronen, U. Hager, J. Hakala, A. Jokinen, A. Kankainen, I. Moore, H. Penttila, S. Rinta-Antila, A. Saastamoinen, T. Sonoda, J. Äystö, N. Adimi, G. de France, J.-C. Thomas, G. Voltolini, and T. Chaventre, *Eur. Phys. J. A* **36**, 121 (2008).
- [36] M. Bencomo, J. C. Hardy, V. E. Iacob, H. I. Park, L. Chen, V. Horvat, N. Nica, B. T. Roeder, A. Saastamoinen, and I. S. Towner, *Phys. Rev. C* **100**, 015503 (2019).
- [37] B. Blank, G. Savard, J. Doring, A. Blazhev, G. Canchel, M. Chartier, D. Henderson, Z. Janas, R. Kirchner, I. Mukha, E. Roeckl, K. Schmidt, and J. Zylicz, *Phys. Rev. C* **69**, 015502 (2004).
- [38] K. Blaum, G. Audi, D. Beck, G. Bollen, C. Guenaut, P. Delahaye, F. Herfurth, A. Kellerbauer, H.-J. Kluge, D. Lunney, D. Rodriguez, S. Schwarz, L. Schweikhard, C. Weber, and C. Yazidjian, *Nucl. Phys. A* **746**, 305c (2004).
- [39] B. Blank, A. Bey, I. Matea, J. Souin, L. Audirac, M. J. G. Borge, G. Canchel, P. Delahaye, F. Delaee, C.-E. Dumonchy, R. Dominguez-Reyes, L. M. Fraile, J. Giovinazzo, T. T. Hui, J. Huikari, D. Lunney, F. Munoz, J.-L. Pedroza, C. Plaisir, L. Scrani, S. Sturm, O. Tengblad, and F. Wenender, *Eur. Phys. J. A* **44**, 363 (2010).
- [40] B. Blank, J.-C. Thomas, P. Ascher, L. Audirac, A. Bacquias, L. Cáceres, G. Canchel, L. Daudin, F. de Oliveira Santos, F. Didierjean, M. Gerbaux, J. Giovinazzo, S. Grévy, T. Kurtukian Nieto, I. Matea, F. Munoz, M. Roche, L. Serani, N. Smirnova, and J. Souin, *Eur. Phys. J. A* **51**, 8 (2015).
- [41] R. O. Bondelid and J. W. Butler, *Nucl. Phys.* **53**, 618 (1964).
- [42] S. A. Brindhaban and P. H. Barker, *Phys. Rev. C* **49**, 2401 (1994); reference replaces earlier conference proceedings from the same laboratory.
- [43] R. H. Burch, C. A. Gagliardi, and R. E. Tribble, *Phys. Rev. C* **38**, 1365 (1988).
- [44] J. T. Burke, P. A. Vetter, S. J. Freedman, B. K. Fujikawa, and W. T. Winter, *Phys. Rev. C* **74**, 025501 (2006).
- [45] G. Canchel, B. Blank, M. Chartier, F. Delaee, P. Dendooven, C. Dossat, J. Giovinazzo, J. Huikari, A. S. Lalleman, M. J. Lopez Jimenez, V. Madec, J. L. Pedroza, H. Penttila, and J. C. Thomas, *Eur. Phys. J. A* **23**, 409 (2005).
- [46] N. M. Chaudri, *Fizika* **16**, 297 (1984).
- [47] L. Chen, J. C. Hardy, M. Bencomo, V. Horvat, N. Nica, and H. I. Park, *Nucl. Instrum. Methods A* **728**, 81 (2013).
- [48] J. Chen and B. Singh, *Nucl. Data Sheets* **135**, 1 (2016).
- [49] G. J. Clark, J. M. Freeman, D. C. Robinson, J. S. Ryder, W. E. Burcham, and G. T. A. Squier, *Nucl. Phys. A* **215**, 429 (1973); this reference replaces the half-life value in *Phys. Lett. B* **35**, 503 (1971).
- [50] C. N. Davids, in *Atomic Masses and Fundamental Constants 6*, edited by J. A. Nolen and W. Benenson (Plenum, New York, 1980), p. 419.
- [51] W. W. Daehnick and R. D. Rosa, *Phys. Rev. C* **31**, 1499 (1985).
- [52] P. De Wit and C. Van der Leun, *Phys. Lett. B* **30**, 639 (1969).
- [53] R. M. DelVecchio and W. W. Daehnick, *Phys. Rev. C* **17**, 1809 (1978).
- [54] M. A. van Driel, H. Klijman, G. A. P. Engelbertink, H. H. Eggehuysen, and J. A. J. Hermans, *Nucl. Phys. A* **240**, 98 (1975).
- [55] R. Dunlop, G. C. Ball, J. R. Leslie, C. E. Svensson, I. S. Towner, C. Andreoiu, S. Chagnon-Lessard, A. Chester, D. S. Cross, P. Finlay, A. B. Garnsworthy, P. E. Garrett, J. Glister, G. Hackman, B. Hadinia, K. G. Leach, E. T. Rand, K. Starosta, E. R. Tardiff, S. Triambak, S. J. Williams, J. Wong, S. W. Yates, and E. F. Zganjar, *Phys. Rev. C* **88**, 045501 (2013).

- [56] M. R. Dunlop, C. E. Svensson, G. C. Ball, G. F. Grinyer, J. R. Leslie, C. Andreoiu, R. A. E. Austin, T. Ballast, P. C. Bender, V. Bildstein, A. Diaz Varela, R. Dunlop, A. B. Garnsworthy, P. E. Garrett, G. Hackman, B. Hadinia, D. S. Jamieson, A. T. Laffoley, A. D. MacLean, D. M. Miller, W. J. Mills, J. Park, A. J. Radich, M. M. Rajabali, E. T. Rand, C. Unsworth, A. Valencik, Z. M. Wang, and E. F. Zganjar, *Phys. Rev. Lett.* **116**, 172501 (2016).
- [57] M. R. Dunlop, C. E. Svensson, G. C. Ball, J. R. Leslie, C. Andreoiu, N. Bernier, H. Bidaman, V. Bildstein, M. Bowry, C. Burbadge, R. Caballero-Folch, A. D. Varela, R. Dunlop, A. B. Garnsworthy, P. E. Garrett, G. Hackman, B. Jigmeddorj, K. G. Leach, A. D. MacLean, B. Olaizola, J. Measures, C. Natzke, Y. Saito, J. K. Smith, J. Turko, and T. Zidar, *Phys. Rev. C* **96**, 045502 (2017).
- [58] P. M. Endt, P. De Wit, and C. Alderliesten, *Nucl. Phys. A* **476**, 333 (1988).
- [59] T. Eronen, V. Elomaa, U. Hager, J. Hakala, A. Jokinen, A. Kankainen, I. Moore, H. Penttilä, S. Rahaman, S. Rinta-Antila, A. Saastamoinen, T. Sonoda, J. Äystö, A. Bey, B. Blank, G. Canchel, C. Dossat, J. Giovinazzo, I. Matea, and N. Adimi, *Phys. Lett. B* **636**, 191 (2006).
- [60] T. Eronen, V. Elomaa, U. Hager, J. Hakala, A. Jokinen, A. Kankainen, I. Moore, H. Penttilä, S. Rahaman, J. Rissanen, A. Saastamoinen, T. Sonoda, J. Äystö, J. C. Hardy, and V. S. Kolhinen, *Phys. Rev. Lett.* **97**, 232501 (2006).
- [61] T. Eronen, V.-V. Elomaa, U. Hager, J. Hakala, J. C. Hardy, A. Jokinen, A. Kankainen, I. D. Moore, H. Penttilä, S. Rahaman, S. Rinta-Antila, J. Rissanen, A. Saastamoinen, T. Sonoda, C. Weber, and J. Äystö, *Phys. Rev. Lett.* **100**, 132502 (2008).
- [62] T. Eronen, V.-V. Elomaa, U. Hager, J. Hakala, A. Jokinen, A. Kankainen, T. Kessler, I. D. Moore, S. Rahaman, J. Rissanen, C. Weber, and J. Äystö, *Phys. Rev. C* **79**, 032802(R) (2009).
- [63] T. Eronen, V.-V. Elomaa, J. Hakala, J. C. Hardy, A. Jokinen, I. D. Moore, M. Reponen, J. Rissanen, A. Saastamoinen, C. Weber, and J. Äystö, *Phys. Rev. Lett.* **103**, 252501 (2009).
- [64] T. Eronen, D. Gorelov, J. Hakala, J. C. Hardy, A. Jokinen, A. Kankainen, V. S. Kolhinen, I. D. Moore, H. Penttilä, M. Reponen, J. Rissanen, A. Saastamoinen, and J. Äystö, *Phys. Rev. C* **83**, 055501 (2011).
- [65] T. Eronen, J. C. Hardy, L. Canete, A. Jokinen, J. Hakala, A. Kankainen, V. S. Kolhinen, J. Koponen, I. D. Moore, I. M. Murray, H. Penttilä, I. Pohjalainen, O. Polshchuk, J. Reinikainen, S. Rinta-Antila, N. Soukouti, A. Voss, and J. Äystö, *Phys. Rev. C* **95**, 025501 (2017).
- [66] S. Ettenauer, M. C. Simon, A. T. Gallant, T. Brunner, U. Chowdhury, V. V. Simon, M. Brodeur, A. Chaudhuri, E. Mané, C. Andreoiu, G. Audi, J. R. Crespo López-Urrutia, P. Delheij, G. Gwinner, A. Lapierre, D. Lunney, M. R. Pearson, R. Ringle, J. Ullrich, and J. Dilling, *Phys. Rev. Lett.* **107**, 272501 (2011).
- [67] T. Faestermann, R. Hertenberger, H.-F. Wirth, R. Krucken, M. Mahgoub, and P. Maier-Komor, *Eur. Phys. J. A* **42**, 339 (2009).
- [68] P. Finlay, G. C. Ball, J. R. Leslie, C. E. Svensson, I. S. Towner, R. A. E. Austin, D. Bandyopadhyay, A. Chaffey, R. S. Chakrawarthy, P. E. Garrett, G. F. Grinyer, G. Hackman, B. Hyland, R. Kanungo, K. G. Leach, C. M. Mattoon, A. C. Morton, C. J. Pearson, A. A. Phillips, J. J. Ressler, F. Sarazin, H. Savajols, M. A. Schumaker, and J. Wong, *Phys. Rev. C* **78**, 025502 (2008); the branching-ratio result in this reference replaces the result reported in B. Hyland *et al.*, *Phys. Rev. Lett.* **97**, 102501 (2006).
- [69] P. Finlay, S. Ettenauer, G. C. Ball, J. R. Leslie, C. E. Svensson, C. Andreoiu, R. A. E. Austin, D. Bandyopadhyay, D. S. Cross, G. Demand, M. Djongolov, P. E. Garrett, K. L. Green, G. F. Grinyer, G. Hackman, K. G. Leach, C. J. Pearson, A. A. Phillips, C. S. Sumithrarachchi, S. Triambak, and S. J. Williams, *Phys. Rev. Lett.* **106**, 032501 (2011).
- [70] P. Finlay, G. C. Ball, J. R. Leslie, C. E. Svensson, C. Andreoiu, R. A. E. Austin, D. Bandyopadhyay, D. S. Cross, G. Demand, M. Djongolov, S. Ettenauer, P. E. Garrett, K. L. Green, G. F. Grinyer, G. Hackman, K. G. Leach, C. J. Pearson, A. A. Phillips, E. T. Rand, C. S. Sumithrarachchi, S. Triambak, and S. J. Williams, *Phys. Rev. C* **85**, 055501 (2012).
- [71] G. Frick, A. Gallmann, D. E. Alburger, D. H. Wilkinson, and J. P. Coffin, *Phys. Rev.* **132**, 2169 (1963).
- [72] J. M. Freeman, G. Murray, and W. E. Burcham, *Phys. Lett.* **17**, 317 (1965).
- [73] J. M. Freeman, J. G. Jenkin, G. Murray, D. C. Robinson, and W. E. Burcham, *Nucl. Phys. A* **132**, 593 (1969); this reference replaces the half-life values in J. M. Freeman, J. G. Jenkin, G. Murray, and W. E. Burcham, *Phys. Rev. Lett.* **16**, 959 (1966).
- [74] J. M. Freeman, R. J. Petty, S. D. Hoath, G. T. A. Squier, and W. E. Burcham, *Phys. Lett. B* **53**, 439 (1975).
- [75] B. K. Fujikawa, S. J. Asztalos, R. M. Clark, M. A. Deleplanque-Stephens, P. Fallon, S. J. Freeman, J. P. Greene, I.-Y. Lee, L. J. Lising, A. O. Macchiavelli, R. W. MacLeod, J. C. Reich, M. A. Rowe, S.-Q. Shang, F. S. Stephens, and E. G. Wasserman, *Phys. Lett. B* **449**, 6 (1999).
- [76] A. Gallmann, E. Aslanides, F. Jundt, and E. Jacobs, *Phys. Rev.* **186**, 1160 (1969).
- [77] M. Gaelens, J. Andrzejewski, J. Camps, P. Decroock, M. Huysse, K. Kruglov, W. F. Mueller, A. Piechaczek, N. Severijns, J. Szerypo, G. Vancraeynest, P. Van Duppen, and J. Wauters, *Eur. Phys. J. A* **11**, 413 (2001).
- [78] S. George, G. Audi, B. Blank, K. Blaum, M. Breitenfeldt, U. Hager, F. Herfurth, A. Herlert, A. Kellerbauer, H.-J. Kluge, M. Kretschmar, D. Lunney, R. Savreux, S. Schwarz, L. Schweikhard, and C. Yazidjian, *Europhys. Lett.* **82**, 50005 (2008).
- [79] D. R. Goosman and D. E. Alburger, *Phys. Rev. C* **5**, 1893 (1972); the branching-ratio upper limit set in this reference is considered to replace the much higher value reported by D. R. Brown, S. M. Ferguson, and D. H. Wilkinson, *Nucl. Phys. A* **135**, 159 (1969).
- [80] C. A. Grossmann, M. A. LaBonte, G. E. Mitchell, J. D. Shriner, J. F. Shriner, Jr., G. A. Vavrina, and P. M. Wallace, *Phys. Rev. C* **62**, 024323 (2000).
- [81] G. F. Grinyer, P. Finlay, C. E. Svensson, G. C. Ball, J. R. Leslie, R. A. E. Austin, D. Bandyopadhyay, A. Chaffey, R. S. Chakrawarthy, P. E. Garrett, G. Hackman, B. Hyland, R. Kanungo, K. G. Leach, C. M. Mattoon, A. C. Morton, C. J. Pearson, A. A. Phillips, J. J. Ressler, F. Sarazin, H. Savajols, M. A. Schumaker, and J. Wong, *Phys. Rev. C* **77**, 015501 (2008).
- [82] G. F. Grinyer, G. C. Ball, H. Bouzomita, S. Ettenauer, P. Finlay, A. B. Garnsworthy, P. E. Garrett, K. L. Green, G. Hackman, J. R. Leslie, C. J. Pearson, E. T. Rand, C. S. Sumithrarachchi, C. E. Svensson, J. C. Thomas, S. Triambak, and S. J. Williams, *Phys. Rev. C* **87**, 045502 (2013); this reference replaces the half-life value in G. F. Grinyer, M. B.

- Smith, C. Andreoiu, A. N. Andreyev, G. C. Ball, P. Bricault, R. S. Chakravarthy, J. J. Daoud, P. Finlay, P. E. Garrett, G. Hackman, B. Hyland, J. R. Leslie, A. C. Morton, C. J. Pearson, A. A. Phillips, M. A. Schumaker, C. E. Svensson, J. J. Valiente-Dobon, S. J. Williams, and E. F. Zganjar, *ibid.* **76**, 025503 (2007).
- [83] J. C. Hardy and D. E. Alburger, *Phys. Lett. B* **42**, 341 (1972).
- [84] J. C. Hardy, H. Schmeing, J. S. Geiger, and R. L. Graham, *Nucl. Phys. A* **223**, 157 (1974). [This reference replaces results in J. C. Hardy, H. Schmeing, J. S. Geiger, R. L. Graham, and I. S. Towner, *Phys. Rev. Lett.* **29**, 1027 (1972).]
- [85] J. C. Hardy, H. R. Andrews, J. S. Geiger, R. L. Graham, J. A. Macdonald, and H. Schmeing, *Phys. Rev. Lett.* **33**, 1647 (1974).
- [86] J. C. Hardy, G. C. Ball, J. S. Geiger, R. L. Graham, J. A. Macdonald, and H. Schmeing, *Phys. Rev. Lett.* **33**, 320 (1974); the value for the ^{46}V Q_{EC} -value from this reference was later withdrawn by J. C. Hardy and I. S. Towner, in *Atomic Masses and Fundamental Constants 5*, edited by J. H. Sanders and A. H. Wapstra (Plenum, New York, 1976), p. 66.
- [87] J. C. Hardy, H. Schmeing, J. S. Geiger, and R. L. Graham, *Nucl. Phys. A* **246**, 61 (1975). [This reference replaces results in J. C. Hardy, H. Schmeing, J. S. Geiger, R. L. Graham, and I. S. Towner, *Phys. Rev. Lett.* **29**, 1027 (1972).]
- [88] E. Hagberg, V. T. Koslowsky, J. C. Hardy, I. S. Towner, J. G. Hykawy, G. Savard, and T. Shinozuka, *Phys. Rev. Lett.* **73**, 396 (1994); uncertainties on the Gamow-Teller decays observed from ^{46}V and ^{50}Mn did not appear in this reference but have been derived from the original data and added here.
- [89] P. D. Harty, N. S. Bowden, P. H. Barker, and P. A. Amundsen, *Phys. Rev. C* **58**, 821 (1998).
- [90] J. C. Hardy and I. S. Towner, *Phys. Rev. Lett.* **88**, 252501 (2002).
- [91] J. C. Hardy, V. E. Iacob, M. Sanchez-Vega, R. G. Neilson, A. Azhari, C. A. Gagliardi, V. E. Mayes, X. Tang, L. Trache, and R. E. Tribble, *Phys. Rev. Lett.* **91**, 082501 (2003).
- [92] D. L. Hendrie and J. B. Gerhart, *Phys. Rev.* **121**, 846 (1961).
- [93] A. M. Hernandez and W. W. Daehnick, *Phys. Rev. C* **24**, 2235 (1981).
- [94] A. M. Hernandez and W. W. Daehnick, *Phys. Rev. C* **25**, 2957 (1982).
- [95] R. G. Helmer and C. van der Leun, *Nucl. Instrum. Methods A* **450**, 35 (2000).
- [96] F. Herfurth, A. Kellerbauer, F. Ames, G. Audi, D. Beck, K. Blaum, G. Bollen, O. Engels, H.-J. Kluge, D. Lunney, R. B. Moore, O. Oinonen, E. Sauvan, C. Scheidenberger, S. Schwarz, G. Sikler, and C. Weber, *Eur. Phys. J. A* **15**, 17 (2002).
- [97] I. Hofmann, *Acta Phys. Austr.* **18**, 309 (1964).
- [98] S. D. Hoath, R. J. Petty, J. M. Freeman, G. T. A. Squier, and W. E. Burcham, *Phys. Lett. B* **51**, 345 (1974).
- [99] P. Hungerford and H. H. Schmidt, *Nucl. Instrum. Methods* **192**, 609 (1982).
- [100] B. C. Hyman, V. E. Iacob, A. Azhari, C. A. Gagliardi, J. C. Hardy, V. E. Mayes, R. G. Neilson, M. Sanchez-Vega, X. Tang, L. Trache, and R. E. Tribble, *Phys. Rev. C* **68**, 015501 (2003).
- [101] B. Hyland, D. Melconian, G. C. Ball, J. R. Leslie, C. E. Svensson, P. Bricault, E. Cunningham, M. Dombisky, G. F. Grinyer, G. Hackman, K. Koopmans, F. Sarazin, M. A. Schumaker, H. C. Scraggs, M. B. Smith, and P. M. Walker, *J. Phys. G: Nucl. Part. Phys.* **31**, S1885 (2005).
- [102] V. E. Iacob, J. C. Hardy, J. F. Brinkley, C. A. Gagliardi, V. E. Mayes, N. Nica, M. Sanchez-Vega, G. Tabacaru, L. Trache, and R. E. Tribble, *Phys. Rev. C* **74**, 055502 (2006).
- [103] V. E. Iacob, J. C. Hardy, V. Golovko, J. Goodwin, N. Nica, H. I. Park, L. Trache, and R. E. Tribble, *Phys. Rev. C* **77**, 045501 (2008).
- [104] V. E. Iacob, J. C. Hardy, A. Banu, L. Chen, V. V. Golovko, J. Goodwin, V. Horvat, N. Nica, H. I. Park, L. Trache, and R. E. Tribble, *Phys. Rev. C* **82**, 035502 (2010).
- [105] V. E. Iacob, J. C. Hardy, L. Chen, V. Horvat, M. Bencomo, N. Nica, H. I. Park, B. T. Roeder, and A. Saastamoinen, *Phys. Rev. C* **97**, 035501 (2018).
- [106] V. E. Iacob, J. C. Hardy, H. I. Park, M. Bencomo, L. Chen, V. Horvat, N. Nica, B. T. Roeder, and A. Saastamoinen, *Phys. Rev. C* **101**, 015504 (2020); the half-life result in this reference replaces the value reported in Ref. [102].
- [107] V. E. Iacob, J. C. Hardy, H. I. Park, M. Bencomo, L. Chen, V. Horvat, N. Nica, B. T. Roeder, A. Saastamoinen, and I. S. Towner, *Phys. Rev. C* **101**, 045504 (2020).
- [108] P. D. Ingalls, J. C. Overley, and H. S. Wilson, *Nucl. Phys. A* **293**, 117 (1977).
- [109] M. A. Islam, T. J. Kennett, S. A. Kerr, and W. V. Prestwich, *Can. J. Phys.* **58**, 168 (1980).
- [110] M. J. Lopez Jimenez, B. Blank, M. Chartier, S. Czajkowski, P. Dessagne, G. de France, J. Giovinazzo, D. Karamanis, M. Lewitowicz, V. Maslov, C. Miede, P. H. Regan, M. Stanoiu, and M. Wiescher, *Phys. Rev. C* **66**, 025803 (2002).
- [111] R. W. Kavanagh, *Nucl. Phys. A* **129**, 172 (1969).
- [112] A. Kellerbauer, G. Audi, D. Beck, K. Blaum, G. Bollen, C. Guenaut, F. Herfurth, A. Herlert, H.-J. Kluge, D. Lunney, S. Schwarz, L. Schweikhard, C. Weber, and C. Yazidjian, *Phys. Rev. C* **76**, 045504 (2007). [This result for the mass of ^{74}Rb is the same as—but more clearly explained than—the result given in A. Kellerbauer, G. Audi, D. Beck, K. Blaum, G. Bollen, B. A. Brown, P. Delahaye, C. Guenaut, F. Herfurth, H.-J. Kluge, D. Lunney, S. Schwarz, L. Schweikhard, and C. Yazidjian, *Phys. Rev. Lett.* **93**, 072502 (2004).]
- [113] S. W. Kikstra, C. van der Leun, S. Raman, E. T. Jurney, and I. S. Towner, *Nucl. Phys. A* **496**, 429 (1989).
- [114] S. W. Kikstra, Z. Guo, C. Van der Leun, P. M. Endt, S. Raman, Walkiewicz, J. W. Starner, E. T. Jurney, and I. S. Towner, *Nucl. Phys. A* **529**, 39 (1991).
- [115] V. T. Koslowsky, E. Hagberg, J. C. Hardy, R. E. Azuma, E. T. H. Clifford, H. C. Evans, H. Schmeing, U. J. Schrewe, and K. S. Sharma, *Nucl. Phys. A* **405**, 29 (1983).
- [116] V. T. Koslowsky, J. C. Hardy, E. Hagberg, R. E. Azuma, G. C. Ball, E. T. H. Clifford, W. G. Davies, H. Schmeing, U. J. Schrewe, and K. S. Sharma, *Nucl. Phys. A* **472**, 419 (1987); the ^{14}O - $^{26}\text{Al}^m$ Q_{EC} -value-difference result reported in this reference replaces an earlier value given in V. T. Koslowsky, J. C. Hardy, R. E. Azuma, G. C. Ball, E. T. H. Clifford, W. G. Davies, E. Hagberg, H. Schmeing, U. J. Schrewe, and K. S. Sharma, *Phys. Lett. B* **119**, 57 (1982).
- [117] V. T. Koslowsky, E. Hagberg, J. C. Hardy, G. Savard, H. Schmeing, K. S. Sharma, and X. J. Sun, *Nucl. Instrum. Methods A* **401**, 289 (1997).
- [118] V. T. Koslowsky, E. Hagberg, J. C. Hardy, H. Schmeing, and I. S. Towner, *Nucl. Phys. A* **624**, 293 (1997).

- [119] M. A. Kroupa, S. J. Freeman, P. H. Barker, and S. M. Ferguson, *Nucl. Instrum. Methods A* **310**, 649 (1991).
- [120] T. Kurtukian Nieto, J. Souin, T. Eronen, L. Audirac, J. Äystö, B. Blank, V.-V. Elomaa, J. Giovinazzo, U. Hager, J. Hakala, A. Jokinen, A. Kankainen, P. Karvonen, T. Kessler, I. D. Moore, H. Penttilä, S. Rahaman, M. Reponen, S. Rinta-Antila, J. Rissanen, A. Saastamoinen, T. Sonoda, and C. Weber, *Phys. Rev. C* **80**, 035502 (2009).
- [121] A. A. Kwiatkowski, A. Chaudhuri, U. Chowdhury, A. T. Gallant, T. D. Macdonald, B. E. Schultz, M. C. Simon, and J. Dilling, *Ann. Phys. (Berlin)* **525**, 529 (2013).
- [122] A. T. Laffoley, C. E. Svensson, C. Andreoiu, R. A. E. Austin, G. C. Ball, B. Blank, H. Bouzomita, D. S. Cross, A. Diaz Varela, R. Dunlop, P. Finlay, A. B. Garnsworthy, P. E. Garrett, J. Giovinazzo, G. F. Grinyer, G. Hackman, B. Hadinia, D. S. Jamieson, S. Ketelhut, K. G. Leach, J. R. Leslie, E. Tardiff, J. C. Thomas, and C. Unsworth, *Phys. Rev. C* **88**, 015501 (2013).
- [123] A. T. Laffoley, C. E. Svensson, C. Andreoiu, G. C. Ball, P. C. Bender, H. Bidaman, V. Bildstein, B. Blank, D. S. Cross, G. Deng, A. D. Varela, M. R. Dunlop, R. Dunlop, A. B. Garnsworthy, P. E. Garrett, J. Giovinazzo, G. F. Grinyer, J. Grinyer, G. Hackman, B. Hadinia, D. S. Jamieson, B. Jigmeddorj, D. Kisliuk, K. G. Leach, J. R. Leslie, A. D. MacLean, D. Miller, B. Mills, M. Moukaddam, A. J. Radich, M. M. Rajabali, E. T. Rand, J. C. Thomas, J. Turko, C. Unsworth, and P. Voss, *Phys. Rev. C* **92**, 025502 (2015).
- [124] K. G. Leach, C. E. Svensson, G. C. Ball, J. R. Leslie, R. A. E. Austin, D. Bandyopadhyay, C. Barton, E. Bassiachvilli, S. Etnenauer, P. Finlay, P. E. Garrett, G. F. Grinyer, G. Hackman, D. Melconian, A. C. Morton, S. Mythili, O. Newman, C. J. Pearson, M. R. Pearson, A. A. Phillips, H. Savajols, M. A. Schumaker, and J. Wong, *Phys. Rev. Lett.* **100**, 192504 (2008).
- [125] S. Lin, S. A. Brindhaban, and P. H. Barker, *Phys. Rev. C* **49**, 3098 (1994).
- [126] P. V. Magnus, E. G. Adelberger, and A. Garcia, *Phys. Rev. C* **49**, R1755 (1994).
- [127] I. Matea, J. Souin, J. Äystö, B. Blank, P. Delahaye, V.-V. Elomaa, T. Eronen, J. Giovinazzo, U. Hager, J. Hakala, J. Huikari, A. Jokinen, A. Kankainen, I. D. Moore, J.-L. Pedroza, S. Rahaman, J. Rissanen, J. Ronkainen, A. Saastamoinen, T. Sonoda, and C. Weber, *Eur. Phys. J. A* **37**, 151 (2008); I. Matea, *ibid.* **38**, 247(E) (2008).
- [128] C. E. Moss, C. Detraz, and C. S. Zaidins, *Nucl. Phys. A* **174**, 408 (1971).
- [129] F. Molina, B. Rubio, Y. Fujita, W. Gelletly, J. Agramunt, A. Algora, J. Benlliure, P. Boutachkov, L. Cáceres, R. B. Cakirli, E. Casarejos, C. Domingo-Pardo, P. Doornenbal, A. Gadea, E. Ganioglu, M. Gascón, H. Geissel, J. Gerl, M. Górská, J. Grębosz, R. Hoischen, R. Kumar, N. Kurz, I. Kojouharov, L. A. Susam, H. Matsubara, A. I. Morales, Y. Oktem, D. Pauwels, D. Pérez-Loureiro, S. Pietri, Z. Podolyák, W. Prokopowicz, D. Rudolph, H. Schaffner, S. J. Steer, J. L. Tain, A. Tamii, S. Taschenov, J. J. Valiente-Dobón, S. Verma, and H.-J. Wollersheim, *Phys. Rev. C* **91**, 014301 (2015).
- [130] A. I. Morales, A. Algora, B. Rubio, K. Kaneko, S. Nishimura, P. Aguilera, S. E. A. Orrigo, F. Molina, G. de Angelis, F. Recchia, G. Kiss, V. H. Phong, J. Wu, D. Nishimura, H. Oikawa, T. Goigoux, J. Giovinazzo, P. Asche, J. Agramunt, D. S. Ahn, H. Baba, B. Blank, C. Borcea, A. Boso, P. Davies, F. Diel, Zs. Dombrádi, P. Doornenbal, J. Eberth, G. de France, Y. Fujita, N. Fukuda, E. Ganioglu, W. Gelletly, M. Gerbaux, S. Grévy, V. Guadilla, N. Inabe, T. Isobe, I. Kojouharov, W. Korten, T. Kubo, S. Kubono, T. Kurtukiám Nieto, N. Kurz, J. Lee, S. Lenzi, J. Liu, T. Lokotko, D. Lubos, C. Magron, A. Montaner-Pizá, D. R. Napoli, H. Sakurai, H. Schaffner, Y. Shimizu, C. Sidong, P.-A. Söderström, T. Sumikama, H. Suzuki, H. Takeda, Y. Takei, M. Tanaka, and S. Yagi, *Phys. Rev. C* **95**, 064327 (2017).
- [131] M. Mukherjee, A. Kellerbauer, D. Beck, K. Blaum, G. Bollen, F. Carrel, P. Delahaye, J. Dilling, S. George, C. Guenaut, F. Herfurth, A. Herlert, H.-J. Kluge, U. Koster, D. Lunney, S. Schwarz, L. Schweikhard, and C. Yazidjian, *Phys. Rev. Lett.* **93**, 150801 (2004).
- [132] Y. Nagai, K. Kunihiro, T. Toriyama, S. Harada, Y. Torii, A. Yoshida, T. Nomura, J. Tanaka, and T. Shinozuka, *Phys. Rev. C* **43**, R9 (1991).
- [133] M. Oinonen, J. Äystö, P. Baumann, J. Cederkäll, S. Courtin, P. Dessagne, S. Franchoo, H. Fynbo, M. Górská, J. Huikari, A. Jokinen, A. Knipper, U. Köster, G. LeScornet, C. Miehé, A. Nieminen, T. Nilsson, Yu. Novikov, K. Peräjärvi, E. Poirier, A. Popov, D. M. Seliverstov, T. Siiskonen, H. Simon, O. Tengblad, P. Van Duppen, G. Walter, L. Weissman, and K. Wilhelmsen-Rolander, *Phys. Lett. B* **511**, 145 (2001).
- [134] T. K. Onishi, A. Gelberg, H. Sakurai, K. Yoneda, N. Aoi, N. Imai, H. Baba, P. von Brentano, N. Fukuda, Y. Ichikawa, M. Ishihara, H. Iwasaki, D. Kameda, T. Kishida, A. F. Lisetskiy, H. J. Ong, M. Osada, T. Otsuka, M. K. Suzuki, K. Ue, Y. Utsuno, and H. Watanabe, *Phys. Rev. C* **72**, 024308 (2005).
- [135] H. I. Park, J. C. Hardy, V. E. Jacob, A. Banu, L. Chen, V. V. Golovko, J. Goodwin, V. Horvat, N. Nica, E. Simmons, L. Trache, and R. E. Tribble, *Phys. Rev. C* **84**, 065502 (2011).
- [136] H. I. Park, J. C. Hardy, V. E. Jacob, L. Chen, J. Goodwin, N. Nica, E. Simmons, L. Trache, and R. E. Tribble, *Phys. Rev. C* **85**, 035501 (2012).
- [137] H. I. Park, J. C. Hardy, V. E. Jacob, M. Bencomo, L. Chen, V. Horvat, N. Nica, B. T. Roeder, E. Simmons, R. E. Tribble, and I. S. Towner, *Phys. Rev. Lett.* **112**, 102502 (2014).
- [138] H. I. Park, J. C. Hardy, V. E. Jacob, M. Bencomo, L. Chen, V. Horvat, N. Nica, B. T. Roeder, E. McCleskey, R. E. Tribble, and I. S. Towner, *Phys. Rev. C* **92**, 015502 (2015).
- [139] A. Piechaczek, E. F. Zganjar, G. C. Ball, P. Bricault, J. M. D'Auria, J. C. Hardy, D. F. Hodgson, V. Jacob, P. Klages, W. D. Kulp, J. R. Leslie, M. Lipoglavsek, J. A. Macdonald, H.-B. Mak, D. M. Moltz, G. Savard, J. von Schwarzenberg, C. E. Svensson, I. S. Towner, and J. L. Wood, *Phys. Rev. C* **67**, 051305(R) (2003); the branching-ratio results from this measurement are considered to replace the contradictory upper limit set in an earlier less-precise measurement [133].
- [140] F. W. Prosser, G. U. Din, and D. D. Tolbert, *Phys. Rev.* **157**, 779 (1967).
- [141] W. V. Prestwich and T. J. Kennett, *Can. J. Phys.* **68**, 261 (1990); **68**, 1352(E) (1990).
- [142] S. Raman, E. T. Jurney, D. A. Outlaw, and I. S. Towner, *Phys. Rev. C* **27**, 1188 (1983).
- [143] I. Reusen, A. Andreyev, J. Andzrejewski, N. Bijmens, S. Franchoo, M. Huyse, Yu. Kudryavtsev, K. Kruglov, W. F. Mueller, A. Piechaczek, R. Raabe, K. Rykaczewski, J. Szerypo, P. Van Duppen, L. Vermeeren, J. Wauters, and A. Wöhr, *Phys. Rev. C* **59**, 2416 (1999).

- [144] M. P. Reiter, K. G. Leach, O. M. Drozdowski, S. R. Stroberg, J. D. Holt, C. Andreoiu, C. Bbcock, B. Barquest, M. Brodeur, A. Finlay, M. Foster, A. T. Gallant, G. Gwinner, R. Klawitter, B. Kootte, A. A. Kwiatkowski, Y. Lan, D. Lascar, E. Leistenschneider, A. Lennarz, S. Paul, R. Steinbrügge, R. I. Thompson, M. Wieser, and J. Dilling, *Phys. Rev. C* **96**, 052501(R) (2017).
- [145] D. C. Robinson, J. M. Freeman, and T. T. Thwaites, *Nucl. Phys. A* **181**, 645 (1972); this reference replaces the ^{10}C branching ratio from J. M. Freeman, J. G. Jenkin, and G. Murray, *ibid.* **124**, 393 (1969).
- [146] D. C. Robinson and P. H. Barker, *Nucl. Phys. A* **225**, 109 (1974).
- [147] C. Rolfs, W. S. Rodney, S. Durrance, and H. Winkler, *Nucl. Phys. A* **240**, 221 (1975).
- [148] D. Rodriguez, G. Audi, J. Äystö, D. Beck, K. Blaum, G. Bollen, F. Herfurth, A. Jokinen, A. Kellerbauer, H.-J. Kluge, V. S. Kohlinen, M. Oinonen, E. Sauvan, and S. Schwarz, *Nucl. Phys. A* **769**, 1 (2006). [This result for the mass of ^{74}Kr is the same as but more clearly explained than the result given in A. Kellerbauer, G. Audi, D. Beck, K. Blaum, G. Bollen, B. A. Brown, P. Delahaye, C. Guenaut, F. Herfurth, H.-J. Kluge, D. Lunney, S. Schwarz, L. Schweikhard, and C. Yazidjian, *Phys. Rev. Lett.* **93**, 072502 (2004).]
- [149] J. S. Ryder, G. J. Clark, J. E. Draper, J. M. Freeman, W. E. Burcham, and G. T. A. Squier, *Phys. Lett. B* **43**, 30 (1973).
- [150] A. M. Sandorfi, C. J. Lister, D. E. Alburger, and E. K. Warburton, *Phys. Rev. C* **22**, 2213 (1980).
- [151] G. Savard, A. Galindo-Uribarri, E. Hagberg, J. C. Hardy, V. T. Koslowsky, D. C. Radford, and I. S. Towner, *Phys. Rev. Lett.* **74**, 1521 (1995).
- [152] G. Savard, J. A. Clark, F. Buchinger, J. E. Crawford, S. Gulick, J. C. Hardy, A. A. Hecht, V. E. Jacob, J. K. P. Lee, A. F. Levand, B. F. Lundgren, N. D. Scielzo, K. S. Sharma, I. Tanihata, I. S. Towner, W. Trimble, J. C. Wang, Y. Wang, and Z. Zhou, *Phys. Rev. C* **70**, 042501(R) (2004).
- [153] G. Savard, F. Buchinger, J. A. Clark, J. E. Crawford, S. Gulick, J. C. Hardy, A. A. Hecht, J. K. P. Lee, A. F. Levand, N. D. Scielzo, H. Sharma, K. S. Sharma, I. Tanihata, A. C. C. Villari, and Y. Wang, *Phys. Rev. Lett.* **95**, 102501 (2005).
- [154] J. Savory, P. Schury, C. Bachelet, M. Block, G. Bollen, M. Facina, C. M. Folden III, C. Guénaut, E. Kwan, A. A. Kwiatkowski, D. J. Morrissey, G. K. Pang, A. Prinke, R. Ringle, H. Schatz, S. Schwarz, and C. S. Sumithrarachchi, *Phys. Rev. Lett.* **102**, 132501 (2009).
- [155] P. Schury, C. Bachelet, M. Block, G. Bollen, D. A. Davies, M. Facina, C. M. Folden III, C. Guénaut, J. Huikari, E. Kwan, A. Kwiatkowski, D. J. Morrissey, R. Ringle, G. K. Pang, A. Prinke, J. Savory, H. Schatz, S. Schwarz, C. S. Sumithrarachchi, and T. Sun, *Phys. Rev. C* **75**, 055801 (2007).
- [156] R. J. Scott, G. J. O'Keefe, M. N. Thompson, and R. P. Rassool, *Phys. Rev. C* **84**, 024611 (2011).
- [157] J. C. Sens, A. Pape, and R. Armbruster, *Nucl. Phys. A* **199**, 241 (1973).
- [158] G. S. Sidhu and J. B. Gerhart, *Phys. Rev.* **148**, 1024 (1966).
- [159] J. Singh, *Ind. J. Pure Appl. Phys.* **10**, 289 (1972).
- [160] J. Souin, T. Eronen, P. Ascher, L. Audirac, J. Äystö, B. Blank, V.-V. Elomaa, J. Giovanazzo, J. Hakala, A. Jokinen, V. S. Kolhinen, P. Karvonen, I. D. Moore, S. Rahaman, J. Rissanen, A. Saastamoinen, and J. C. Thomas, *Eur. Phys. J. A* **47**, 40 (2011).
- [161] G. T. A. Squier, W. E. Burcham, J. M. Freeman, R. J. Petty, S. D. Hoath, and J. S. Ryder, *Nucl. Phys. A* **242**, 62 (1975).
- [162] V. T. Takau, M. N. Thompson, R. J. Scott, R. P. Rassool, and G. J. O'Keefe, *Radiat. Phys. Chem.* **81**, 1669 (2012).
- [163] N. R. Tolich, P. H. Barker, P. D. Harty, and P. A. Amundsen, *Phys. Rev. C* **67**, 035503 (2003).
- [164] I. S. Towner and J. C. Hardy, *Phys. Rev. C* **72**, 055501 (2005).
- [165] R. E. Tribble, J. D. Cossairt, D. P. May, and R. A. Kenefick, *Phys. Rev. C* **16**, 917 (1977).
- [166] A. A. Valverde, G. Bollen, M. Brodeur, R. A. Bryce, K. Cooper, M. Eibach, K. Gulyuz, C. Izzo, D. J. Morrissey, M. Redshaw, R. Ringle, R. Sandler, S. Schwarz, C. S. Sumithrarachchi, and A. C. C. Villari, *Phys. Rev. Lett.* **114**, 232502 (2015).
- [167] H. Vonach, P. Glaessel, E. Huenges, P. Maier-Komor, H. Roesler, H. J. Scheerer, H. Paul, and D. Semrad, *Nucl. Phys. A* **278**, 189 (1977).
- [168] P. A. Voytas, E. A. George, G. W. Severin, L. Zhan, and L. D. Knutson, *Phys. Rev. C* **92**, 065502 (2015).
- [169] E. K. Warburton, J. W. Olness, and A. R. Poletti, *Phys. Rev.* **160**, 938 (1967).
- [170] F. B. Waanders, J. P. L. Reinecke, H. N. Jacobs, J. J. A. Smit, M. A. Meyer, and P. M. Endt, *Nucl. Phys. A* **411**, 81 (1983).
- [171] T. A. Walkiewicz, S. Raman, E. T. Journey, J. W. Starner, and J. E. Lynn, *Phys. Rev. C* **45**, 1597 (1992).
- [172] M. Wang, G. Audi, F. G. Kondev, W. J. Huang, S. Naimi and X. Xu, *Chin. Phys. C* **41**, 030003 (2017).
- [173] R. E. White, H. Naylor, P. H. Barker, D. M. J. Lovelock, and R. M. Smythe, *Phys. Lett. B* **105**, 116 (1981).
- [174] R. E. White, P. H. Barker, and D. M. J. Lovelock, *Metrologia* **21**, 193 (1985).
- [175] D. H. Wilkinson and D. E. Alburger, *Phys. Rev. C* **13**, 2517 (1976).
- [176] D. H. Wilkinson, A. Gallmann, and D. E. Alburger, *Phys. Rev. C* **18**, 401 (1978).
- [177] H. S. Wilson, R. W. Kavanagh, and F. M. Mann, *Phys. Rev. C* **22**, 1696 (1980).
- [178] P. Zhang, X. Xu, P. Shuai, R. J. Chen, X. L. Yan, Y. H. Zhang, M. Wang, Yu. A. Litvinov, K. Blaum, H. S. Xu, T. Bao, X. C. Chen, H. Chen, C. Y. Fu, J. J. He, S. Kubono, Y. H. Lam, D. W. Liu, R. S. Mao, X. W. Ma, M. Z. Sun, X. L. Tu, Y. M. Xing, J. C. Yang, Y. J. Yuan, Q. Zeng, X. Zhou, X. H. Zhou, W. L. Zhan, S. Litvinov, G. Audi, T. Uesaka, Y. Yamaguchi, T. Yamaguchi, A. Ozawa, B. H. Sun, Y. Sun, and F. R. Xu, *Phys. Lett. B* **767**, 20 (2017).
- [179] Y. H. Zhang, P. Zhang, X. H. Zhou, M. Wang, Yu. A. Litvinov, H. S. Xu, X. Xu, P. Shuai, Y. H. Lam, R. J. Chen, X. L. Yan, T. Bao, X. C. Chen, H. Chen, C. Y. Fu, J. J. He, S. Kubono, D. W. Liu, R. S. Mao, X. W. Ma, M. Z. Sun, X. L. Tu, Y. M. Xing, Q. Zeng, X. Zhou, W. L. Zhan, S. Litvinov, K. Blaum, G. Audi, T. Uesaka, Y. Yamaguchi, T. Yamaguchi, A. Ozawa, B. H. Sun, Y. Sun, and F. R. Xu, *Phys. Rev. C* **98**, 014319 (2018).
- [180] J. Zioni, A. A. Jaffe, E. Friedman, N. Haik, R. Schectman, and D. Nir, *Nucl. Phys. A* **181**, 465 (1972).
- [181] F. Zijderhand, R. C. Markus, and C. van der Leun, *Nucl. Phys. A* **466**, 280 (1987).
- [182] M. Tanabashi *et al.* (Particle Data Group), *Phys. Rev. D* **98**, 030001 (2018).

- [183] J. C. Hardy, L. C. Carraz, B. Jonson, and P. G. Hansen, *Phys. Lett. B* **71**, 307 (1977).
- [184] W. J. Marciano and A. Sirlin, *Phys. Rev. Lett.* **56**, 22 (1986); *Phys. Rev. D* **29**, 75 (1984).
- [185] A. Sirlin, *Phys. Rev.* **164**, 1767 (1967).
- [186] W. J. Marciano and A. Sirlin, *Phys. Rev. Lett.* **96**, 032002 (2006).
- [187] C.-Y. Seng, M. Gorchtein, H. H. Patel, and M. J. Ramsey-Musolf, *Phys. Rev. Lett.* **121**, 241804 (2018).
- [188] C.-Y. Seng, M. Gorchtein, and M. J. Ramsey-Musolf, *Phys. Rev. D* **100**, 013001 (2019).
- [189] A. Czarnecki, W. J. Marciano, and A. Sirlin, *Phys. Rev. D* **100**, 073008 (2019).
- [190] A. Sirlin, *Phys. Rev. D* **35**, 3423 (1987).
- [191] A. Sirlin and R. Zucchini, *Phys. Rev. Lett.* **57**, 1994 (1986).
- [192] I. S. Towner and J. C. Hardy, *Phys. Rev. C* **77**, 025501 (2008).
- [193] I. S. Towner and J. C. Hardy, *Phys. Rev. C* **92**, 055505 (2015).
- [194] I. S. Towner, *Phys. Lett. B* **333**, 13 (1994).
- [195] W. Jaus and G. Rasche, *Phys. Rev. D* **41**, 166 (1990).
- [196] I. S. Towner, *Nucl. Phys. A* **540**, 478 (1992).
- [197] M. Gorchtein, *Phys. Rev. Lett.* **123**, 042503 (2019).
- [198] I. S. Towner and J. C. Hardy, *Phys. Rev. C* **82**, 065501 (2010).
- [199] W. Satula, P. Baczyk, J. Dobaczewski, and M. Konieczka, *Phys. Rev. C* **94**, 024306 (2016).
- [200] W. Satula, J. Dobaczewski, W. Nazarewicz, and T. R. Werner, *Phys. Rev. C* **86**, 054316 (2012).
- [201] L. Xayavong and N. A. Smirnova, *Phys. Rev. C* **97**, 024324 (2018).
- [202] I. Angeli and K. P. Marinova, *At. Data Nucl. Data Tables* **99**, 69 (2013).
- [203] V. Tishchenko *et al.* (MuLan Collaboration), *Phys. Rev. D* **87**, 052003 (2013).
- [204] I. S. Towner and J. C. Hardy, in *Symmetries and Fundamental Interactions in Nuclei*, edited by W. C. Haxton and E. M. Henley (World Scientific, Singapore, 1995), pp. 183–249.
- [205] I. S. Towner and J. C. Hardy, in *Proceedings of the V International WEIN Symposium: Physics Beyond the Standard Model, Santa Fe, NM 1998*, edited by P. Herzeg, C. M. Hoffman, and H. V. Klapdor-Kleingrothaus (World Scientific, Singapore, 1999), pp. 338–359.
- [206] M. Antonelli *et al.*, *Eur. Phys. J. C* **69**, 399 (2010).
- [207] V. Cirigliano, M. Moulson, and E. Passemar, The status of V_{us} , presentation given at *Current and Future Status of First-Row CKM Unitarity*, UMass Amherst (2019), https://www.physics.umass.edu/acfi/sites/acfi/files/slides/moulson_amherst.pdf.
- [208] D. Giusti, V. Lubicz, C. Tarantino, G. Martinelli, C. T. Sachrajda, F. Sanfilippo, S. Simula, and N. Tantalo, *Phys. Rev. Lett.* **120**, 072001 (2018).
- [209] M. Di Carlo, G. Martinelli, D. Giusti, V. Lubicz, C. T. Sachrajda, F. Sanfilippo, S. Simula, and N. Tantalo, *Phys. Rev. D* **100**, 034514 (2019).
- [210] E. Blucher and W. J. Marciano, V_{us} , V_{ud} , the Cabibbo Angle, and CKM Unitarity, minireview for the Particle Data Group (2018); see Ref. [182].
- [211] S. Aoki *et al.* [Flavor Lattice Averaging Group (FLAG)], *Eur. Phys. J. C* **80**, 113 (2020).
- [212] J. D. Jackson, S. B. Treiman, and H. W. Wyld, Jr., *Phys. Rev.* **106**, 517 (1957).
- [213] H. Behrens and W. Bühring, *Electron Radial Wave Functions and Nuclear Beta-decay* (Clarendon Press, Oxford, UK, 1982).
- [214] B. Blank *et al.*, *Eur. Phys. J. A* **56**, 156 (2020).